Eur. Phys. J. C (2017) 77:467
DOI 10.1140/epjc/s10052-017-5030-3

THE EUROPEAN PHYSICAL JOURNAL C

Regular Article - Experimental Physics

Measurement of the jet mass in highly boosted $t\bar{t}$ events from pp collisions at $\sqrt{s} = 8$ TeV

CMS Collaboration*

CERN, 1211 Geneva 23, Switzerland

Received: 18 March 2017 / Accepted: 27 June 2017 / Published online: 14 July 2017

Abstract The first measurement of the jet mass m_{jet} of top quark jets produced in $t\bar{t}$ events from pp collisions at $\sqrt{s} = 8$ TeV is reported for the jet with the largest transverse momentum p_{T} in highly boosted hadronic top quark decays. The data sample, collected with the CMS detector, corresponds to an integrated luminosity of 19.7 fb^{-1}. The measurement is performed in the lepton+jets channel in which the products of the semileptonic decay $t \to bW$ with $W \to \ell\nu$ where ℓ is an electron or muon, are used to select $t\bar{t}$ events with large Lorentz boosts. The products of the fully hadronic decay $t \to bW$ with $W \to q\bar{q}'$ are reconstructed using a single Cambridge–Aachen jet with distance parameter $R = 1.2$, and $p_{\text{T}} > 400$ GeV. The $t\bar{t}$ cross section as a function of m_{jet} is unfolded at the particle level and is used to test the modelling of highly boosted top quark production. The peak position of the m_{jet} distribution is sensitive to the top quark mass m_{t}, and the data are used to extract a value of m_{t} to assess this sensitivity.

1 Introduction

The top quark may play a special role in the standard model (SM) of particle physics owing to its large mass and its possible importance in electroweak symmetry breaking [1,2]. Measurements of $t\bar{t}$ production provide crucial information about the accuracy of the SM near the electroweak scale [3,4], and in assessing the predictions of quantum chromodynamics (QCD) at large mass scales. In turn, they can be used to determine the fundamental parameters of the theory, such as the strong coupling constant or the top quark mass [5,6].

Previous differential measurements of the $t\bar{t}$ production cross section [7–15] at the Fermilab Tevatron and CERN LHC show excellent agreement with SM predictions. However, investigations of top quarks with very large transverse momenta p_{T} have proven to be difficult, since in this kinematic range the decays of the top quark to fully hadronic final states become highly collimated and merge into single jets. In this highly boosted regime, the $t\bar{t}$ reconstruction efficiency deteriorates for previous, more-traditional measurements. Special reconstruction techniques based on jet substructure are often used to improve the measurements [16,17] or to implement searches for new physics [18–28]. A detailed understanding of jet substructure observables, and especially the jet mass m_{jet}, is crucial for LHC analyses of highly boosted topologies. While measurements of m_{jet} corrected to the particle level have been carried out for light-quark and gluon jets [29,30], the m_{jet} distribution for highly boosted top quarks has not yet been measured.

Apart from testing the simulation of m_{jet} in fully hadronic top quark decays, the location of the peak of the m_{jet} distribution is sensitive to the top quark mass m_{t} [31]. This measurement therefore provides an alternative method of determining m_{t} in the boosted regime, independent of previous mass measurements [32–37]. Calculations from first principles have been performed in soft collinear effective theory [38–41] for the dijet invariant mass distribution from highly boosted top quark production in e^+e^- collisions [42,43], and work is ongoing to extend this to the LHC environment [44,45]. Such calculations account for perturbative and nonperturbative effects, and provide particle-level predictions. Once predictions for the LHC become available, the measurement of the m_{jet} distribution can lead to an extraction of m_{t} without the ambiguities that arise from the unknown relation between m_{t} in a well-defined renormalisation scheme and the top quark mass parameter used in Monte Carlo (MC) simulations [45–48].

We present the first measurement of the differential $t\bar{t}$ production cross section as a function of the leading-jet mass, where leading refers to the jet with the highest p_{T}. The measurement is based on data from pp collisions at $\sqrt{s} = 8$ TeV, recorded by the CMS experiment at the LHC in 2012 and corresponding to an integrated luminosity of 19.7 fb^{-1}. It is performed on $t\bar{t}$ events in which the leading jet includes all $t \to bW^+ \to bq\bar{q}'$ decay products. The other top quark is required to decay through the semileptonic

* e-mail: cms-publication-committee-chair@cern.ch

mode $\bar{t} \to \bar{b}W^- \to \bar{b}\ell\bar{\nu}_\ell$, where ℓ can be either an electron or muon. The use of charge-conjugate modes is implied throughout this article. The semileptonic top quark decay serves as a means for selecting $t\bar{t}$ events without biasing the m_{jet} distribution from the fully hadronic top quark decay. The highly boosted top quark jets used in the measurement are defined through the Cambridge–Aachen (CA) jet-clustering algorithm [49,50] with a distance parameter $R = 1.2$ and $p_{\text{T}} > 400$ GeV. The m_{jet} distribution is unfolded to the particle level and compared to predictions from MC simulations. The measurement is also normalised to a fiducial-region total cross section defined below, and shows the expected sensitivity to the value of m_{t}. An extraction of the value of m_{t} is performed to assess the overall sensitivity of the measurement.

2 The CMS detector

The central feature of the CMS detector is a superconducting solenoid of 6 m internal diameter, providing a magnetic field of 3.8 T. A silicon pixel and strip tracker, a lead tungstate crystal electromagnetic calorimeter (ECAL), and a brass and scintillator hadron calorimeter (HCAL), each composed of a barrel and two endcap sections reside within the magnetic volume. In addition to the barrel and endcap detectors, CMS has extensive forward calorimetry. Muons are detected using four layers of gas-ionization detectors embedded in the steel flux-return yoke of the magnet. The inner tracker measures charged particle trajectories within the pseudorapidity range $|\eta| < 2.5$. A two-stage trigger system [51] is used to select for analysis pp collisions of scientific interest. A more detailed description of the CMS detector, together with a definition of the coordinate system and relevant kinematic variables, can be found in Ref. [52].

3 Event reconstruction

The CMS experiment uses a particle-flow (PF) event reconstruction [53,54], which aggregates input from all subdetectors. This information includes charged particle tracks from the tracking system and energies deposited in the ECAL and HCAL, taking advantage of the granularity of the subsystems. Particles are classified as electrons, muons, photons, and charged and neutral hadrons. Primary vertices are reconstructed using a deterministic annealing filter algorithm [55]. The vertex with the largest sum in the associated track p_{T}^2 values is taken to be the primary event vertex.

Muons are detected and measured in the pseudorapidity range $|\eta| < 2.1$ using the information collected in the muon and tracking detectors [56]. Tracks from muon candidates must be consistent with a muon originating from the primary event vertex, and satisfy track-fit quality requirements [57].

Electrons are reconstructed in the range $|\eta| < 2.1$, by combining tracking information with energy deposits in the ECAL [58,59]. Electron candidates are required to originate from the primary event vertex. Electrons are identified through the information on the energy distribution in their shower, the track quality, the spatial match between the track and electromagnetic cluster, and the fraction of total cluster energy in the HCAL. Electron candidates that are consistent with originating from photon conversions in the detector material are rejected.

Since the top quark decay products can be collimated at high values of top quark p_{T}, no isolation requirements on the leptons are imposed in either the trigger or in the offline selections (see Sect. 4). The imbalance in event $\mathbf{p_T}$ is quantified as the missing transverse momentum vector $\mathbf{p}_{\text{T}}^{\text{miss}}$, defined as the projection on the plane perpendicular to the beams of the negative vector sum of the momenta of all PF candidates in the event. Its magnitude is referred to as $p_{\text{T}}^{\text{miss}}$.

The PF candidates are clustered into jets by using the FastJet 3.0 software package [60]. Charged hadrons associated with event vertices other than the primary event vertex are removed prior to jet clustering. Isolated leptons (either electron or muon) are not part of the input list for jet finding [53,54]. Small-radius jets are clustered with the anti-k_{T} jet-clustering algorithm [61] with a distance parameter $R = 0.5$ (AK5 jets). These small-radius jets are used at the trigger level, in the first steps of the event selection, and for the identification of jets coming from the hadronisation of b quarks. If a nonisolated lepton candidate is found within the angular distance $\Delta R < 0.5$ of an AK5 jet, its four-momentum is subtracted from that of the jet to avoid double counting of energy and ensure proper jet energy corrections. The angular distance is given by $\Delta R = \sqrt{(\Delta\phi)^2 + (\Delta\eta)^2}$, where $\Delta\phi$ and $\Delta\eta$ are the differences in azimuthal angle (in radians) and pseudorapidity, respectively, between the directions of the lepton and jet. Large-radius jets are obtained by using the CA jet-clustering algorithm [49,50] with $R = 1.2$ (CA12 jets). When a lepton candidate is found among the PF candidates clustered into a CA12 jet, its four-momentum is subtracted from that of the CA12 jet. In this paper, the unmodified term "jet" will refer to the broad CA12 jets.

All jets could contain neutral particles from additional pp collisions in the same or nearby beam crossings (pileup). This extra contribution is subtracted based on the average expectation of the pileup in the jet catchment area [62]. This is done by calculating a correction for the average offset energy density in each event as a function of the number of primary vertices [63,64]. The AK5 jets are identified as originating from the fragmentation of a b quark with the combined secondary vertex algorithm (CSV) [65]. A tight operating point

is used, which has a misidentification probability of 0.1% for tagging light-parton jets with an average p_T of about 80 GeV, and an efficiency of about 50% for a heavy-flavour jet with p_T in the range 50–160 GeV. Above 160 GeV, the efficiency decreases gradually to about 30% for a p_T value of 400 GeV [65]. All jets are required to satisfy quality selections to minimize the impact of calorimeter noise and other sources of misidentified jets [66]. Events are also required to satisfy selection criteria to remove events with large values of p_T^{miss} from calorimeter noise, as described in Ref. [67].

The jet mass m_{jet} is calculated from the four-vectors p_i of all i PF particles clustered into a jet:

$$m_{jet}^2 = \Big(\sum_{i \text{ in jet}} p_i \Big)^2, \quad (1)$$

where the pion mass is assigned to all charged hadrons. The reconstruction of m_{jet} for CA12 jets is studied by using a sample of highly boosted $W \to q\bar{q}'$ decays merged into a single jet, as described in Sect. 5.5.

4 Trigger and data

The data were recorded by using single-lepton triggers with no isolation requirement applied to the leptons. Events in the muon+jets channel use a trigger that requires at least one muon with $p_T > 40$ GeV and $|\eta| < 2.1$. The efficiency for this trigger, measured in a $Z \to \mu^+\mu^-$ sample, is 95% for muons measured within $|\eta| < 0.9$, 85% for muons within $0.9 < |\eta| < 1.2$, and 83% for $1.2 < |\eta| < 2.1$.

The trigger for the electron+jets channel requires at least one electron with $p_T > 30$ GeV in conjunction with two AK5 jets that have $p_T > 100$ and > 25 GeV, for the leading and next-to-leading AK5 jet, respectively. Events are also included if triggered by a single AK5 jet with $p_T > 320$ GeV. The additional events obtained through this single-jet trigger often contain an electron merged into a jet that cannot be resolved at the trigger stage. The resulting combined trigger efficiency is 90% for events with a leading AK5 jet with $p_T < 320$ GeV. Above this value, the trigger has a turn-on behaviour and is fully efficient above a value of 350 GeV. The trigger efficiencies are measured in data and simulation using a tag-and-probe method in $Z/\gamma^*(\to \ell\ell)$+jets and dileptonic $t\bar{t}$ events. Small differences between data and simulation are corrected for by applying scale factors to the simulated events.

Top quark events, produced via the strong and electroweak interactions, are simulated with the next-to-leading-order (NLO) generator POWHEG 1.380 [68–72] with a value of $m_t = 172.5$ GeV. The $W(\to \ell\nu)$+jets and $Z/\gamma^*(\to \ell\ell)$+jets processes are simulated with MADGRAPH 5.1.5.11 [73], where MADSPIN [74] is used for the decay of heavy resonances. Diboson production processes (WW, WZ, and ZZ) are simulated with PYTHIA 6.424 [75]. Simulated multijet samples are generated in MADGRAPH, but constitute a negligible background. For the estimation of systematic uncertainties, additional $t\bar{t}$ samples are generated with MC@NLO v3.41 [76] or with MADGRAPH for seven values of m_t ranging from 166.5 to 178.5 GeV.

All the samples generated in MADGRAPH and POWHEG are interfaced with PYTHIA 6 for parton showering and fragmentation (referred to as MADGRAPH+PYTHIA and POWHEG+PYTHIA, respectively). The MLM algorithm [77] used in MADGRAPH is applied during the parton matching to avoid double counting of parton configurations. The MADGRAPH samples use the CTEQ6L [78] parton distribution functions (PDFs). The POWHEG $t\bar{t}$ sample uses the CT10 [79] PDFs, whereas the single top quark processes use the CTEQ6M [80] PDFs. The PYTHIA 6 Z2* tune [81,82] is used to model the underlying event. Top quark events produced with MC@NLO use the CTEQ6M PDF set and HERWIG 6.520 [83] for parton showering and fragmentation (MC@NLO+HERWIG). The default HERWIG tune is used to model the underlying event.

The normalisations of the simulated event samples are taken from the NLO calculations of their cross sections that contain the next-to-next-to-leading-logarithm (NNLL) soft-gluon resummations for single top quark production [84], the next-to-next-to-leading-order (NNLO) calculations for $W(\to \ell\nu)$+jets and $Z/\gamma^*(\to \ell\ell)$+jets [85–87], and the NLO calculation for diboson production [88]. The normalisation of the $t\bar{t}$ simulation is obtained from QCD NNLO calculations, again including resummation of NNLL soft-gluon terms [89–95].

A detailed simulation of particle propagation through the CMS apparatus and detector response is performed with GEANT4 v9.2 [96]. For all simulated samples, the hard collision is overlaid with simulated minimum-bias collisions. The resulting events are weighted to reproduce the pileup distribution measured in data. The same event reconstruction software is used for data and simulated events. The resolutions and efficiencies for reconstructed objects are corrected to match those measured in data [56,58,64,65,97].

5 Cross section measurement

5.1 Strategy

The measurement is carried out in the ℓ+jets channel, which allows the selection of a pure $t\bar{t}$ sample because of its distinct signature at large top quark boosts. The measurement is based on choosing kinematic quantities that do not bias the m_{jet} distribution from fully hadronic top quark decays. A bias would be introduced by, e.g. selecting the leading

jet based on the number of subjets, or requiring a certain maximum value of the N-subjettiness [98,99], as applied in common top quark tagging algorithms [100–104]. Such a selection would lead to a distinct three-prong structure of the jet and thus reject events with one quark being soft or collinear with respect to the momentum of the top quark decay.

The fiducial region chosen for this investigation is studied through simulations at the particle level (defined by all particles with lifetimes longer than 10^{-8} s). The exact selection is detailed below. It relies on having a highly boosted semileptonic top quark decay, where the lepton from $W \to \ell\nu_\ell$ is close in ΔR to the jet from the hadronisation of the accompanying b quark (b jet). A second high-p_T jet is selected, which is assumed to originate from the fully hadronic top quark decay. A veto on additional jets is employed, which ensures that the fully hadronic decay is merged into a single jet. The jet veto is also beneficial for calculating higher-order terms, as it suppresses the size of nonglobal logarithms [105], which appear because of the sensitivity of the jet mass to radiation in only a part of the phase space [106]. The event selection at the reconstruction level is chosen to ensure high efficiency while reducing non-$t\bar{t}$ backgrounds. Finally, the m_{jet} distribution is unfolded for experimental effects and then compared to different MC predictions at the particle level. A measurement of the normalised m_{jet} distribution is performed as well, where the normalisation is performed by using the total measured $t\bar{t}$ cross section in the fiducial phase-space region.

5.2 Definition of the fiducial phase space

The $t\bar{t}$ cross section as a function of the mass of the leading jet is unfolded to the particle level, correcting for experimental effects, with the fiducial phase space at the particle level defined through the selection described below.

As mentioned previously, the measurement is performed in the ℓ+jets channel, where ℓ refers to an electron or muon from the W boson decay. The τ lepton decays are not considered as part of the signal. Leptons are required to be within $|\eta| < 2.1$ and have $p_T > 45$ GeV. Jets are clustered by using the CA algorithm with a distance parameter $R = 1.2$ and required to have $|\eta| < 2.5$. The value of R is chosen to optimize the relationship between obtaining a sufficient number of events and maintaining a narrow width in the jet-mass distribution. The four-momentum of the leading lepton is subtracted from the four-momentum of a jet if the lepton is found within an angular range of $\Delta R < 1.2$ of the jet axis. Events are selected if at least one jet has $p_{T,1} > 400$ GeV and a second jet has $p_{T,2} > 150$ GeV. The leading jet in p_T is assumed to originate from the $t \to Wb \to q\bar{q}'b$ decay, merged into a single jet. Consequently, the second jet is considered to originate from the fragmented b quark

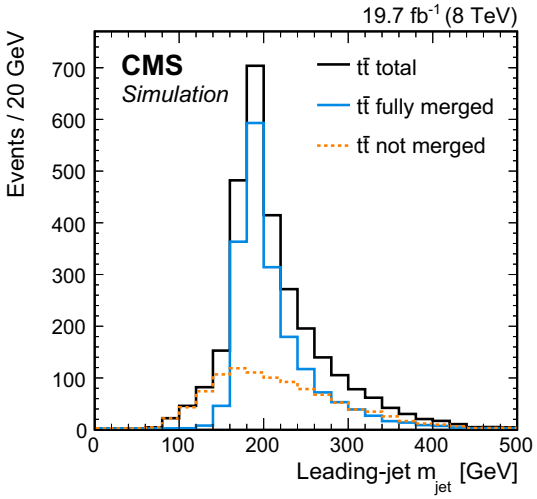

Fig. 1 Simulated mass distributions of the leading jet in $t\bar{t}$ events for the ℓ+jets channel at the particle level. The events are generated with POWHEG+PYTHIA, and normalised to the integrated luminosity of the data. The distribution for the total number of selected events (*dark solid line*) is compared to events where the leading jet originates from the fully hadronic top quark decay (*light solid line*, "fully merged"), and to events where the leading jet does not include all the remnants (*dotted line*, "not merged") from the fully hadronic top quark decay

of the semileptonic top quark decay. To select events with a highly boosted topology, a veto is employed on additional jets with $p_{T,veto} > 150$ GeV. The jet veto removes about 16% of the signal events, but increases the fraction of fully merged top quark decays to about 40%, where an event is called fully merged if the maximum distance in ΔR between the leading jet at the particle level and each individual parton from the fully hadronic top quark decay is smaller than 1.2.

Two additional selection criteria are introduced to ensure that the leading jet includes all particles from the fully hadronic top quark decay. The angular difference $\Delta R(\ell, j_2)$ between the lepton and the second jet has to be smaller than 1.2. This, together with the veto on additional jets, ensures that the top quarks are produced back-to-back in the transverse plane. In addition, the invariant mass of the leading jet has to be greater than the invariant mass of the combination of the second jet and the lepton, $m_{jet,1} > m_{jet,2+\ell}$. This improves the choice of the leading jet as originating from the fully hadronic top quark decay.

The simulated distribution of the jet mass at the particle level after this selection is shown in Fig. 1. The distribution of all jets passing the particle-level selection is compared to distributions in jet mass from fully merged and not merged $t\bar{t}$ decays. After the selection outlined above, jets that do not originate from fully merged top quark decays with a fully hadronic final state are expected to constitute about 35% of all jets in the final data sample, as determined by using the POWHEG+PYTHIA simulation.

5.3 Selection of events at the reconstruction level

A selection is applied at the reconstruction level to obtain an enriched $\mathrm{t\bar{t}}$ sample with high-p_T top quarks, based on leptons without an isolation requirement. As a second step, high-p_T jets are required to be kinematically similar to those selected at the particle level. Comparable kinematic properties between the reconstruction and particle levels lead to small bin-to-bin migrations and therefore to small corrections when unfolding the data.

Selected events must contain exactly one muon or electron with $p_\mathrm{T} > 45\,\mathrm{GeV}$ and $|\eta| < 2.1$. Events with more than one lepton are vetoed to suppress contributions from dileptonic $\mathrm{t\bar{t}}$ decays. To select highly boosted $\mathrm{t\bar{t}}$ events, at least one AK5 jet is required to have $p_\mathrm{T} > 150\,\mathrm{GeV}$ and another AK5 jet $p_\mathrm{T} > 50\,\mathrm{GeV}$, where both jets have to fulfil $|\eta| < 2.4$. The suppression of background from multijet production is accomplished by using a two-dimensional (2D) isolation variable that is efficient at large top quark boosts, yet notably reduces multijet background. This 2D isolation requires the angular difference between the lepton and the nearest AK5 jet directions $\Delta R_\mathrm{min}(\mathrm{lepton, jets})$ to be greater than 0.5, or the perpendicular component of the lepton momentum relative to the nearest AK5 jet $p_\mathrm{rel,T}$ to be larger than 25 GeV. In the calculation of these quantities, only AK5 jets with $p_\mathrm{T} > 25\,\mathrm{GeV}$ are considered. The efficiency of the 2D isolation requirement has been studied in data and simulation by using $\mathrm{Z}/\gamma^*(\rightarrow \ell\ell)$+jets events [26].

A requirement on $p_\mathrm{T}^\mathrm{miss} > 20\,\mathrm{GeV}$ and on the scalar sum $p_\mathrm{T}^\mathrm{miss} + p_\mathrm{T}^\ell > 150\,\mathrm{GeV}$ reduces the contribution from multijet and $\mathrm{Z}/\gamma^*(\rightarrow \ell\ell)$+jets production, where p_T^ℓ is the lepton transverse momentum. Given the presence of two b quarks in the events, at least one AK5 jet is required to be identified as originating from the fragmentation of a b quark by using the CSV algorithm, which reduces the contribution from W+jets production. The electron channel includes an additional topological selection criterion to suppress the remaining residual contribution from multijet production:

$$|\Delta\phi(\{\mathrm{e\ or\ jet}\},\ \mathbf{p}_\mathrm{T}^\mathrm{miss}) - 1.5| < p_\mathrm{T}^\mathrm{miss}/50\,\mathrm{GeV},$$

with $\Delta\phi$ measured in radians and $p_\mathrm{T}^\mathrm{miss}$ in GeV. This criterion rejects events in which $\mathbf{p}_\mathrm{T}^\mathrm{miss}$ points along the transverse momentum vector of the leading jet or the lepton. After these requirements, the background contribution from multijet production is negligible.

The selection procedure outlined above results in a $\mathrm{t\bar{t}}$ sample with high purity and selection efficiency at large top quark p_T. In addition, events are selected with kinematic requirements similar to those at the particle level. For each event to pass the selection, at least one jet is required with $p_\mathrm{T} > 400\,\mathrm{GeV}$ and another with $p_\mathrm{T} > 150\,\mathrm{GeV}$, where both jets have to fulfil $|\eta| < 2.5$. Contributions from not fully merged $\mathrm{t\bar{t}}$ events are suppressed with a veto on additional jets with transverse momentum $p_\mathrm{T} > 150\,\mathrm{GeV}$ and $|\eta| < 2.5$. The jet veto has an efficiency of 93% for fully-merged signal events. The fraction of fully merged events with a back-to-back topology is further enhanced by selecting events with an angular difference $\Delta R(\ell, \mathrm{j}_2) < 1.2$ between the directions of the lepton and the subleading jet. To ensure that the leading jet originates from the fully merged top quark decay, its invariant mass is required to be larger than the mass of the subleading jet. With these selection criteria, the reconstruction efficiency for $\mathrm{t\bar{t}}$ events where one top quark decays semileptonically in the fiducial region of the measurement is 23.2%. Several of the above criteria are relaxed in the unfolding procedure to define sideband regions included as additional bins in the response matrix, increasing thereby the reconstruction efficiency.

After the selection procedure, the contribution of non-signal $\mathrm{t\bar{t}}$ events from $\mathrm{t\bar{t}}$ decays to the τ+jets, dilepton, and all-jets channels constitute, respectively, 7.3, 11.6, and 0.4% of the selected events. These contributions are accounted for in the unfolding.

The distributions in p_T and η for the leading jet in selected events are shown in Fig. 2 from data and simulation. The mass distribution of the leading jet at the reconstruction level is shown in Fig. 3 for the p_T regions of $400 < p_\mathrm{T} < 500\,\mathrm{GeV}$ (upper) and $p_\mathrm{T} > 500\,\mathrm{GeV}$ (lower). In these plots the $\mathrm{t\bar{t}}$ simulation is scaled such that the number of simulated events matches the number of selected events observed in data. Overall good agreement between data and the predictions is observed. The slight slope in the data/MC ratio of the jet mass distribution in Fig. 3 (upper) is covered by the jet energy and mass scale uncertainties, as described below.

Table 1 shows the total number of events observed in data together with the total number of signal and background events determined from simulation.

5.4 Unfolding from the reconstruction level to the particle level

The transformation from the reconstruction to the particle level is carried out through a regularised unfolding based on a least-squares fit, implemented in the TUnfold [107] framework. This procedure suppresses the statistical fluctuations by a regularisation with respect to the count in each bin. The optimal regularisation strength is determined through a minimization of the average global correlation coefficient of the output bins [108]. Contributions from background processes such as W+jets, single top quark, and multijet production are determined from simulation and subtracted from the data prior to the unfolding. Non-signal $\mathrm{t\bar{t}}$ events are accounted for in the unfolding by including them in the response matrix, described below.

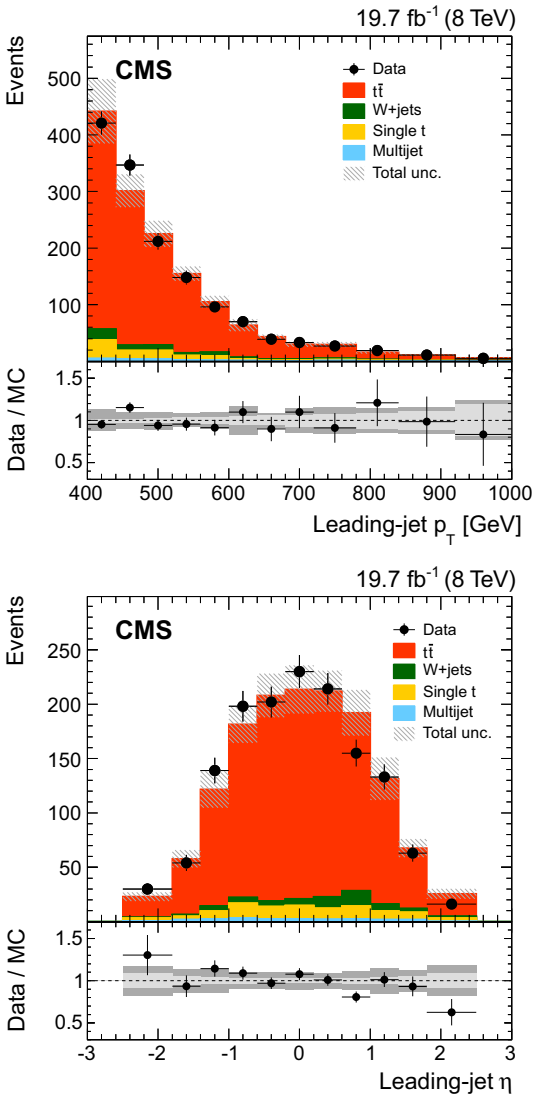

Fig. 2 Distributions of p_{T} (*upper*) and η (*lower*) of the leading jet from data (*points*) and simulation (*filled histograms*). The *vertical bars on the points* show the statistical uncertainty and the *horizontal bars* show the bin widths. The electron and muon channels are shown combined. The *hatched region* shows the total uncertainty in the simulation, including the statistical and experimental systematic uncertainties. The *panels* below show the ratio of the data to the simulation. The uncertainty *bands* include the statistical and experimental systematic uncertainties, where the statistical (*light grey*) and total (*dark grey*) uncertainties are shown separately in the ratio

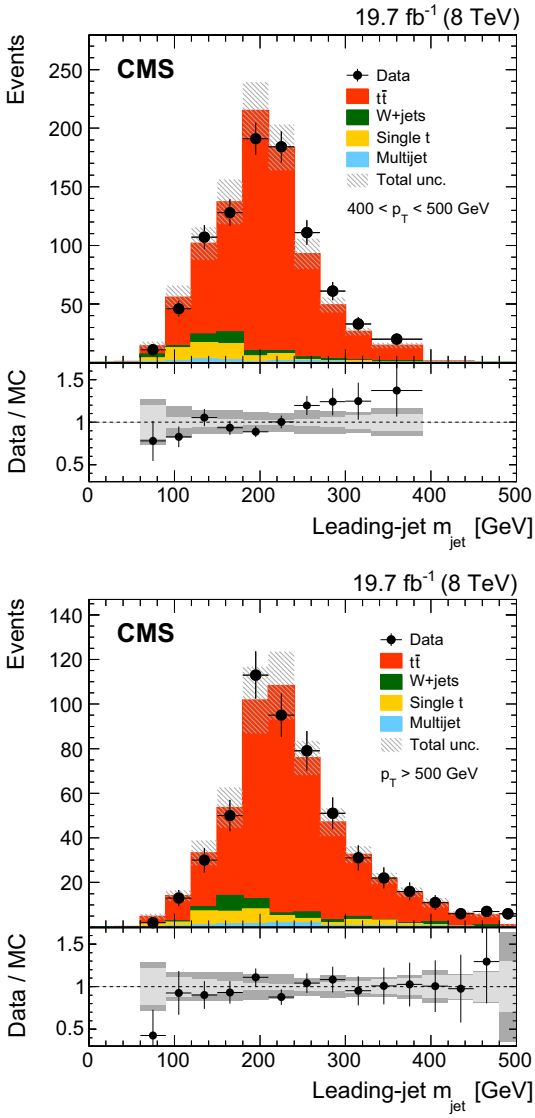

Fig. 3 Distributions of the leading-jet invariant mass from data (*points*) and simulation (*filled histograms*). The *vertical bars on the points* show the statistical uncertainty and the *horizontal bars* show the bin widths for the combined electron and muon channels. The distributions for p_{T} bins of $400 < p_{\mathrm{T}} < 500\,\mathrm{GeV}$ (*upper*) and $p_{\mathrm{T}} > 500\,\mathrm{GeV}$ (*lower*) are given. The *hatched region* shows the total uncertainty in the simulation, including the statistical and experimental systematic uncertainties. The *panels* below show the ratio of the data to the simulation. The uncertainty *bands* include the statistical and experimental systematic uncertainties, where the statistical (*light grey*) and total (*dark grey*) uncertainties are shown separately in the ratio

The response matrix is evaluated by using $\mathrm{t\bar{t}}$ events simulated with POWHEG + PYTHIA. It is obtained for the two regions in the leading-jet p_{T} of $400 < p_{\mathrm{T}} < 500\,\mathrm{GeV}$ and $p_{\mathrm{T}} > 500\,\mathrm{GeV}$. This division is needed to account for the distribution of the p_{T} spectrum. The response matrix includes three additional sideband regions to account for migrations in and out of the phase-space region of the measurement. These are obtained for a lower leading-jet p_{T} of $300 < p_{\mathrm{T}} < 400\,\mathrm{GeV}$, a lower second-leading-jet p_{T} of $100 < p_{\mathrm{T}} < 150\,\mathrm{GeV}$, and a higher veto-jet p_{T} of $150 < p_{\mathrm{T}} < 200\,\mathrm{GeV}$. Events that are reconstructed, but do not pass the particle-level selections, are also included in the response matrix. The electron and muon channels are combined, and the combined distribution is unfolded to ensure a sufficient number of events in the unfolding procedure. The electron and muon channels are also unfolded separately, and the results are compared to verify their consistency.

Table 1 Number of events obtained after applying the full selection. The results are given for the individual sources of background, $t\bar{t}$ signal, and data. The uncertainties correspond to the statistical and systematic components added in quadrature

Source	Number of events
Multijet	21 ± 21
W+jets	60 ± 13
Single top quark	90 ± 21
Total background	171 ± 32
$t\bar{t}$ signal	1410 ± 152
Data	1434

5.5 Uncertainties

5.5.1 Statistical uncertainties

Statistical uncertainties in the unfolding procedure arise from three sources. The dominant source reflects the statistical fluctuations in the input data. Second are the uncertainties from the finite number of simulated events used to calculate the response matrix. The third source reflects the statistical uncertainties in the simulation of the background processes. After the unfolding, a total statistical uncertainty is obtained for each bin of the m_{jet} distribution that includes the effects from all three sources, which are correlated among the individual measurement bins.

5.5.2 Experimental systematic uncertainties

Systematic uncertainties related to experimental effects are evaluated by changing calibration factors and corrections to efficiencies within their corresponding uncertainties. The resulting covariance matrix of the unfolded measurement is computed through standard error propagation. The uncertainties are evaluated by unfolding pseudo-data simulated with MadGraph+pythia. Pseudo-data are preferred over data because of the smaller statistical fluctuations in the estimation of the systematic uncertainties. The change in each parameter that yields the largest variation in the unfolded measurement is taken as the uncertainty owing to that parameter. The following sources of experimental systematic uncertainties are considered.

The applied jet energy corrections (JEC) depend on the p_{T} and η of the individual jets. The JEC are obtained by using anti-k_{T} jets with $R = 0.7$ (AK7) [64], and their use is checked on CA12 jets by using simulated events. Residual differences between generated and reconstructed jet momenta caused by the larger jet size used in this analysis result in increased uncertainties in the JEC by factors of two to four with respect to the AK7 values. Changes of the JEC within their uncertainties are made in the three-momenta of the jets to estimate the effect on the measured cross section. The jet mass is kept fixed to avoid double-counting of uncertainties when including the uncertainty in the jet-mass scale. A smearing is applied in the jet energy resolution (JER) as an η-dependent correction to all jets in the simulation. The corrections are again changed within their uncertainty to estimate the systematic uncertainty related to the JER smearing. The uncertainties are found to be small compared to the ones from the JEC. The jet-mass scale and the corresponding uncertainty in the CA12 jets have been studied in events that contain a $\text{W} \to \text{q}\bar{\text{q}}'$ decay reconstructed as a single jet in $t\bar{t}$ production. The ratio of the reconstructed jet-mass peak positions in data and simulation is 1.015 ± 0.012. No correction to the jet-mass scale is applied, but an uncertainty of 1.5% is assigned, corresponding to the difference in peak positions. The widths of the jet mass distributions are about 15 GeV, consistent between data and simulation.

Corrections in b tagging efficiency are applied as p_{T}-dependent scale factors for each jet flavour. The corresponding systematic uncertainties are obtained by changing the scale factors within their uncertainties. Pileup correction factors are applied to match the number of primary interactions to the instantaneous luminosity profile in data. The uncertainty is obtained by changing the total inelastic cross section by $\pm 5\%$ [109]. Trigger and lepton identification scale factors are used to correct for differences in the lepton selection efficiency between data and simulation. The corresponding uncertainties are computed by changing the scale factors within their uncertainties [56,58].

5.5.3 Normalisation uncertainties

The effects from uncertainties in background processes are calculated by changing the amount of background subtracted prior to the unfolding and propagating the effect to the output. The uncertainty in the W+jets cross section is taken to be 19%, as obtained from a measurement of W+heavy-flavour quark production [110]; an uncertainty of 23% is applied to the single top quark cross section [111]; and an uncertainty of 100% is assumed for multijet production, estimated from the comparison of various kinematic distributions between data and simulation. Uncertainties affecting the overall normalisation are added in quadrature to the total uncertainty after the unfolding. An uncertainty of 2.6% is applied subsequently for the integrated luminosity [112].

5.5.4 Modelling uncertainties

The unfolding is checked for its dependence on the simulation of $t\bar{t}$ production through the use of alternative programs

to generate events. The effect on the measurement is estimated by using one simulation as pseudo-data input to the unfolding, and another for the calculation of the response matrix. The unfolded result is then compared to the particle-level distribution from the simulation used as pseudo-data. Differences between the unfolded result and the truth-level distribution are taken as the modelling uncertainties.

The uncertainty from the choice of MC generator is estimated by unfolding pseudo-data simulated with MADGRAPH+PYTHIA through a response matrix evaluated with POWHEG+PYTHIA. The effect from the choice of the parton-shower simulation is estimated from events generated with MC@NLO+HERWIG.

The dependence on the choice of m_t in the simulation used to correct the data is also checked. While the unfolded measurement is largely independent of the choice of m_t, residual effects from the kinematic properties of the leptons and jets can lead to additional uncertainties. These uncertainties are evaluated by using events simulated with MADGRAPH+PYTHIA for seven values of m_t from 166.5 to 178.5 GeV, as pseudo-data. This range is considered because no measurement of m_t in this kinematic regime exists, and a stable result, independent of the specific choice of m_t, is therefore crucial. For this check, the response matrix is obtained with MADGRAPH+PYTHIA and a value of $m_t = 172.5$ GeV. The envelope of the uncertainty obtained for different values of m_t is used to define an additional modelling uncertainty.

The uncertainty from the uncalculated higher-order terms in the simulation is estimated by changing the choice of the factorisation and renormalisation scales μ_F and μ_R. For this purpose events simulated with POWHEG+PYTHIA are used, where the scales are changed up and down by factors of two relative to their nominal value. This is set to $\mu_F^2 = \mu_R^2 = Q^2$, where the scale of the hard process is defined by $Q^2 = m_t^2 + \sum p_T^2$ with the sum over all additional final-state partons in the matrix-element calculation. Events with varied scales are unfolded through a response matrix obtained with the nominal choice of scales. The uncertainty in the measurement is defined by the largest change found in the study.

Uncertainties from the PDF are evaluated by using the eigenvectors of the CT10 PDF set with the POWHEG+PYTHIA simulation. The resulting differences in the response matrix are propagated to the measurement. The individual uncertainties for each eigenvector are scaled to the 68% confidence level and added in quadrature [79].

5.5.5 Summary of uncertainties

A summary of the relative uncertainties in this measurement is shown in Fig. 4. The largest contribution is from the statistical uncertainties. The experimental systematic uncertainties are far smaller than those from the modelling of $t\bar{t}$ production. The largest uncertainties are expected to improve considerably with more data at higher centre-of-mass energies. Besides a reduction of the statistical uncertainties, an unfolding of the data using finer bins and as a function of more variables will then be possible, which will result in a reduction of the systematic uncertainties from the simulation of $t\bar{t}$ events. More data will also allow for a measurement that uses smaller jet sizes, which will reduce the uncertainties coming from the jet energy and jet mass scales.

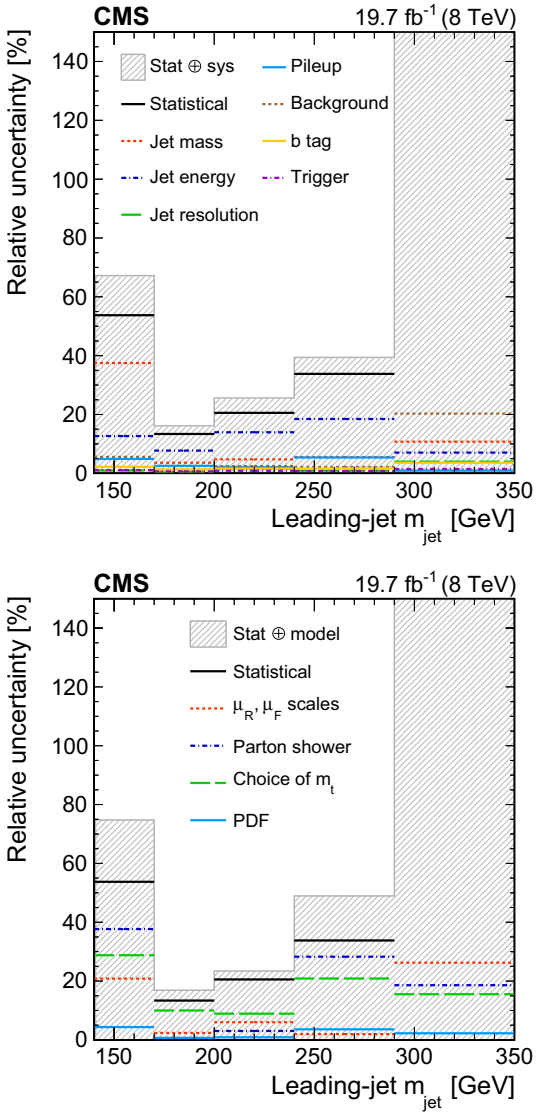

Fig. 4 Statistical uncertainties compared to the individual experimental systematic uncertainties (*upper*), and statistical uncertainties compared to the systematic uncertainties originating from the modelling of $t\bar{t}$ production (*lower*), as a function of the leading-jet mass. The total uncertainties are indicated by the *grey cross-hatched regions*. The statistical and total uncertainties in the last bin are around 300% and exceed the vertical scale. The size of the *horizontal bars* represents the bin widths

Table 2 Summary of the selection criteria used to define the fiducial region of the measurement

Leptons	$p_{\mathrm{T}}^{\ell} > 45\,\mathrm{GeV}$	$\lvert\eta^{\ell}\rvert < 2.1$
Jets	$p_{\mathrm{T},1} > 400\,\mathrm{GeV}$ $p_{\mathrm{T},2} > 150\,\mathrm{GeV}$ $p_{\mathrm{T,veto}} > 150\,\mathrm{GeV}$	$\lvert\eta\rvert < 2.5$
Event	$\Delta R(\ell, \mathrm{j}_2) < 1.2$ $m_{\mathrm{jet},1} > m_{\mathrm{jet},2+\ell}$	

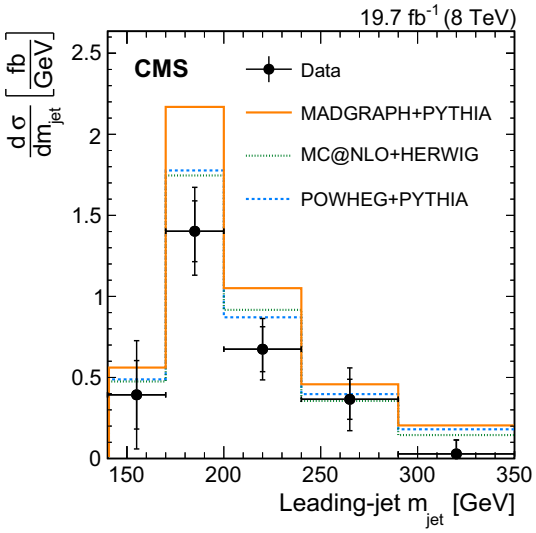

Fig. 5 Fiducial-region particle-level differential $\mathrm{t\bar{t}}$ cross sections as a function of the leading-jet mass. The cross sections from the combined electron and muon channels (*points*) are compared to predictions from the MADGRAPH+PYTHIA, POWHEG+PYTHIA, and MC@NLO+HERWIG generators (*lines*). The *vertical bars* represent the statistical (*inner*) and the total (*outer*) uncertainties. The *horizontal bars* show the bin widths

5.6 Cross section results

The particle-level $\mathrm{t\bar{t}}$ cross section for the fiducial phase-space region is measured differentially as a function of the leading-jet mass in the ℓ+jets channel. The selection criteria defining the fiducial measurement region are summarised in Table 2 (cf. Sect. 5.2).

The measured differential cross section as a function of the leading-jet mass in this fiducial region is shown in Fig. 5, and the numerical values are given in Table 3. The full covariance matrices are given in Appendix A. The data are compared to simulated distributions obtained with POWHEG+PYTHIA, MADGRAPH+PYTHIA, and MC@NLO+HERWIG. The total measured $\mathrm{t\bar{t}}$ cross section for $140 < m_{\mathrm{jet}} < 350\,\mathrm{GeV}$ in the fiducial region is $\sigma = 101 \pm 11\,(\mathrm{stat}) \pm 13\,(\mathrm{syst}) \pm 9\,(\mathrm{model})\,\mathrm{fb}$, where the last uncertainty is from the modelling of the $\mathrm{t\bar{t}}$ signal. Combining all the uncertainties in quadrature gives a value of $\sigma = 101 \pm 19\,\mathrm{fb}$. The predicted fiducial-region cross sections from the MADGRAPH+PYTHIA and POWHEG+PYTHIA $\mathrm{t\bar{t}}$ simulations, assuming a total $\mathrm{t\bar{t}}$ cross section of 253 pb [89–95], are $159\,^{+17}_{-18}$ and $133\,^{+18}_{-28}$ fb, respectively, where the uncertainties are systematic and come from the variations of μ_{R} and μ_{F}. The predictions exceed the measurements, consistent with previously measured $\mathrm{t\bar{t}}$ cross sections at large top quark p_{T} [16,17]. A similar trend is observed when comparing the data to the prediction from MC@NLO+HERWIG. Recent NNLO calculations [113] of the top quark p_{T} spectrum alleviate this discrepancy.

The normalised differential cross section $(1/\sigma)(\mathrm{d}\sigma/\mathrm{d}m_{\mathrm{jet}})$ is obtained by dividing the differential cross sections by the total cross section in the m_{jet} range from 140 to 350 GeV. The result is shown in Fig. 6, together with the predictions of MADGRAPH+PYTHIA for three values of m_{t}. The numerical values of the measured particle-level cross sections are given in Table 4, together with the individual and total uncertainties. The covariance matrices of the measurement are given in Appendix A. The data are well described by the simulation, showing that the overall modelling of the top quark jet mass is acceptable, once the disagreement with the total cross section at large p_{T} is eliminated by the normalisation. The sensitivity of the measurement to m_{t} is clearly visible, albeit compromised by the overall uncertainties.

6 Sensitivity to the top quark mass

Calculations of m_{jet} for $\mathrm{t\bar{t}}$ production from first principles, by using a well-defined definition of m_{t} and not relying on parton shower and hadronisation models, are not yet available for the LHC. Still, a determination of the top quark mass parameter in general-purpose event generators that uses the normalised particle-level cross sections provides a proof of

Table 3 Measured particle-level $\mathrm{t\bar{t}}$ differential cross sections in the fiducial region as a function of m_{jet}, with the individual and total uncertainties in percent

Range in m_{jet} (GeV)	140–170	170–200	200–240	240–290	290–350
Integrated cross section (fb)	12	42	27	18	1.7
Statistical uncertainty (%)	54	13	21	34	300
Systematic uncertainty (%)	40	9	16	20	25
Model uncertainty (%)	52	10	11	35	36
Total uncertainty (%)	85	19	28	53	300

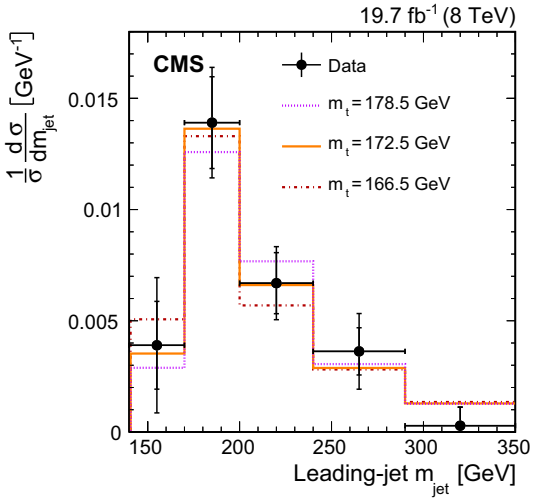

Fig. 6 The normalised particle-level $\mathrm{t\bar{t}}$ differential cross section in the fiducial region as a function of the leading-jet mass. The measurement is compared to predictions from MADGRAPH+PYTHIA for three values of m_t. The *vertical bars* represent the statistical (*inner*) and the total (*outer*) uncertainties. The *horizontal bars* show the bin widths

principle for the feasibility of the method, a cross-check on other determinations of m_t, and an estimate of the current measurement's sensitivity. The value of m_t is determined from the normalised differential cross section measurements given in Table 4, since only the shape of the m_jet distribution can be reliably calculated. Correlations are taken into account through the full covariance matrix of the measurement, which is given in Appendix A. Theoretical predictions are obtained from MADGRAPH+PYTHIA for different values of m_t. A fit is performed based on the χ^2 evaluated as $\chi^2 = d^T V^{-1} d$, where d is the vector of differences between the measured normalised cross sections and the predictions, and V is the covariance matrix, which includes the statistical, experimental systematic, modelling, and theoretical uncertainties. The latter are calculated by changing up and down by factors of two the scales μ_R and μ_F in the MADGRAPH+PYTHIA simulation. The resulting uncertainties are added to the covariance matrix. The χ^2 values obtained for different values of m_t are fitted by a second-order polynomial to determine the minimum, and the uncertainty is determined by a change in χ^2 of 1.0. The result is

$$m_\mathrm{t} = 170.8 \pm 6.0\,(\mathrm{stat}) \pm 2.8\,(\mathrm{syst}) \pm 4.6\,(\mathrm{model}) \pm 4.0\,(\mathrm{theo})\,\mathrm{GeV} \quad (2)$$

$$= 170.8 \pm 9.0\,\mathrm{GeV}, \quad (3)$$

where the total uncertainty in Eq. (3) is the sum in quadrature of the individual uncertainties in Eq. (2). The fit has a minimum χ^2 of 1.6 for three degrees of freedom. This measurement is the first determination of m_t from boosted $\mathrm{t\bar{t}}$ production, calibrated to the MADGRAPH+PYTHIA simulation. It is consistent with recent determinations of m_t that use MC event generators [33,35–37], cross section measurements [6,34,114], and indirect constraints from electroweak fits [115].

7 Summary and outlook

The first measurement of the differential $\mathrm{t\bar{t}}$ cross section has been performed in the ℓ+jets channel as a function of the leading-jet mass m_jet in the highly boosted top quark regime. The measurement is carried out in a fiducial region with fully merged top quark decays in hadronic final states, corrected to the particle level. The normalised differential cross section as a function of m_jet agrees with predictions from simulations, indicating the good quality of modelling the jet mass in highly boosted top quark decays. The total fiducial-region cross section for m_jet between 140 and 350 GeV is measured to be 101 ± 19 fb, which is below the predicted value. This difference is consistent with earlier measurements of a softer top quark p_T spectrum observed in data than in simulation [16,17]. This measurement is a first step towards measuring unfolded jet substructure distributions in highly boosted top quark decays. A detailed understanding of these is crucial for measurements and searches for new physics making use of top quark tagging algorithms.

The peak position in the m_jet distribution is sensitive to the top quark mass m_t. This can be used for an independent determination of m_t in the boosted regime, with the prospect of reaching a more reliable correspondence between the top quark mass in any well-defined renormalisation scheme and the top quark mass parameter in general-purpose event generators.

Table 4 Values of the particle-level $\mathrm{t\bar{t}}$ differential cross section in the fiducial region, normalized to unity, as a function of the leading-jet mass. The individual and total uncertainties are given in percent

Range in m_jet (GeV)	140–170	170–200	200–240	240–290	290–350
Integrated normalised cross section	0.12	0.42	0.27	0.18	0.017
Statistical uncertainty (%)	51	15	21	29	290
Systematic uncertainty (%)	34	5	9	13	27
Model uncertainty (%)	48	9	10	34	36
Total uncertainty (%)	78	18	25	47	300

The normalised particle-level $t\bar{t}$ differential cross section measurement as a function of m_{jet} is used to extract a value of m_{t} in order to estimate the current sensitivity of the data. The value obtained, $m_{\text{t}} = 170.8 \pm 9.0\,\text{GeV}$, is consistent with the current LHC and Tevatron average of $173.34 \pm 0.27\,(\text{stat}) \pm 0.71\,(\text{syst})\,\text{GeV}$ [116], albeit with a much larger uncertainty.

New data at higher centre-of-mass energies and with larger integrated luminosities will lead to an improvement in the statistical uncertainty. More data can also lead to reductions in the experimental systematic uncertainties, most notably that from the jet mass scale, which is expected to improve with smaller jet distance parameters. In addition, improvements in the modelling uncertainty are expected because of stronger constraints on the simulation in the highly boosted regime. A reduction in the theoretical uncertainty is also foreseen with the emergence of higher-order calculations. The results obtained in this analysis show the feasibility of the method to obtain the top quark mass in the highly boosted regime. This can provide an important ingredient for studies of the relation between the value of the top quark mass obtained from MC event generators and the one obtained from first-principle calculations.

Acknowledgements We congratulate our colleagues in the CERN accelerator departments for the excellent performance of the LHC and thank the technical and administrative staffs at CERN and at other CMS institutes for their contributions to the success of the CMS effort. In addition, we gratefully acknowledge the computing centres and personnel of the Worldwide LHC Computing Grid for delivering so effectively the computing infrastructure essential to our analyses. Finally, we acknowledge the enduring support for the construction and operation of the LHC and the CMS detector provided by the following funding agencies: BMWFW and FWF (Austria); FNRS and FWO (Belgium); CNPq, CAPES, FAPERJ, and FAPESP (Brazil); MES (Bulgaria); CERN; CAS, MoST, and NSFC (China); COLCIENCIAS (Colombia); MSES and CSF (Croatia); RPF (Cyprus); SENESCYT (Ecuador); MoER, ERC IUT, and ERDF (Estonia); Academy of Finland, MEC, and HIP (Finland); CEA and CNRS/IN2P3 (France); BMBF, DFG, and HGF (Germany); GSRT (Greece); OTKA and NIH (Hungary); DAE and DST (India); IPM (Iran); SFI (Ireland); INFN (Italy); MSIP and NRF (Republic of Korea); LAS (Lithuania); MOE and UM (Malaysia); BUAP, CINVESTAV, CONACYT, LNS, SEP, and UASLP-FAI (Mexico); MBIE (New Zealand); PAEC (Pakistan); MSHE and NSC (Poland); FCT (Portugal); JINR (Dubna); MON, RosAtom, RAS, RFBR and RAEP (Russia); MESTD (Serbia); SEIDI, CPAN, PCTI and FEDER (Spain); Swiss Funding Agencies (Switzerland); MST (Taipei); ThEPCenter, IPST, STAR, and NSTDA (Thailand); TUBITAK and TAEK (Turkey); NASU and SFFR (Ukraine); STFC (UK); DOE and NSF (USA). Individuals have received support from the Marie-Curie programme and the European Research Council and EPLANET (European Union); the Leventis Foundation; the A. P. Sloan Foundation; the Alexander von Humboldt Foundation; the Belgian Federal Science Policy Office; the Fonds pour la Formation à la Recherche dans l'Industrie et dans l'Agriculture (FRIA-Belgium); the Agentschap voor Innovatie door Wetenschap en Technologie (IWT-Belgium); the Ministry of Education, Youth and Sports (MEYS) of the Czech Republic; the Council of Science and Industrial Research, India; the HOMING PLUS programme of the Foundation for Polish Science, cofinanced from European Union, Regional Development Fund, the Mobility Plus programme of the Ministry of Science and Higher Education, the National Science Center (Poland), contracts Harmonia 2014/14/M/ST2/00428, Opus 2014/13/B/ST2/02543, 2014/15/B/ST2/03998, and 2015/19/B/ST2/02861, Sonata-bis 2012/07/E/ST2/01406; the National Priorities Research Program by Qatar National Research Fund; the Programa Clarín-COFUND del Principado de Asturias; the Thalis and Aristeia programmes cofinanced by EU-ESF and the Greek NSRF; the Rachadapisek Sompot Fund for Postdoctoral Fellowship, Chulalongkorn University and the Chulalongkorn Academic into Its 2nd Century Project Advancement Project (Thailand); and the Welch Foundation, contract C-1845.

A Covariance matrices

The covariance matrices that involve just the statistical components, and the ones involving the total uncertainty (i.e. the statistical, experimental systematic, and modelling uncertainties) are provided in this appendix. All experimental, as well as the PDF and parton-shower uncertainties, are treated as fully correlated in the calculation of the covariance matrices. The uncertainties in the renormalisation and factorisation scale include correlations in the first three bins, and the uncertainties coming from the choice of m_{t} are treated as uncorrelated. Bins 1 to 5 correspond to the following ranges in m_{jet}: 140–170, 170–200, 200–240, 240–290, and 290–350 GeV. The covariance matrices for the differential m_{jet} measurement are given in Tables 5 and 6 for the statistical and total uncertainties, respectively. The covariance matrices for the normalised measurement are given in Tables 7 and 8. Note that the covariance matrices of the normalised measurement are singular, and only four out of the five measurement bins are used in the determination of m_{t}.

Table 5 Covariance matrix for the statistical uncertainties in the differential cross section. All entries are given in units of (fb^2)

Bin	1	2	3	4	5
1	+40.1	−4.3	−8.0	−0.2	−0.6
2		+31.7	−1.5	−8.1	+0.8
3			+30.7	+1.0	−4.5
4				+38.1	+7.3
5					+26.2

Table 6 Covariance matrix for the total uncertainties in the differential cross section, including all systematic and modelling uncertainties. All entries are given in units of (fb^2)

Bin	1	2	3	4	5
1	+100.4	+10.4	−0.3	−22.5	+1.6
2		+66.1	+11.0	+1.4	+0.8
3			+57.4	+12.0	−4.7
4				+93.8	+5.3
5					+26.7

Table 7 Covariance matrix for the statistical uncertainties in the normalised differential cross section. All entries are given in units of (10^{-4})

Bin	1	2	3	4	5
1	+35.0	−11.2	−13.0	−6.7	−4.2
2		+38.3	+0.7	−17.2	−10.6
3			+30.1	−6.0	−11.8
4				+28.1	+1.8
5					+24.8

Table 8 Covariance matrix for the total uncertainties in the normalised differential cross section, including all systematic and modelling uncertainties. All entries are given in units of (10^{-4})

Bin	1	2	3	4	5
1	+83.2	−18.9	−21.0	−40.7	−2.6
2		+55.5	−2.6	−23.7	−10.4
3			+43.1	−7.4	−12.0
4				+72.4	−0.5
5					+25.4

References

1. C.T. Hill, E.H. Simmons, Strong dynamics and electroweak symmetry breaking. Phys. Rept. **381**, 235 (2003). doi:10.1016/S0370-1573(03)00140-6. arXiv: hep-ph/0203079. **(Erratum: Phys. Rept. 390, 553 (2004))**
2. G. Degrassi et al., Higgs mass and vacuum stability in the Standard Model at NNLO. JHEP **08**, 098 (2012). doi:10.1007/JHEP08(2012)098. arXiv:1205.6497
3. A. Buckley et al., Global fit of top quark effective theory to data. Phys. Rev. D **92**, 091501 (2015). doi:10.1103/PhysRevD.92.091501. arXiv:1506.08845
4. A. Buckley et al., Constraining top quark effective theory in the LHC run II era. JHEP **04**, 015 (2016). doi:10.1007/JHEP04(2016)015. arXiv:1512.03360
5. CMS Collaboration, Determination of the top-quark pole mass and strong coupling constant from the $t\bar{t}$ production cross section in pp collisions at $\sqrt{s} = 7$ TeV. Phys. Lett. B **728**, 496 (2013). doi:10.1016/j.physletb.2013.12.009. arXiv:1307.1907. **(Erratum: doi:10.1016/j.physletb.2014.08.040)**
6. CMS Collaboration, Measurement of the $t\bar{t}$ production cross section in the eμ channel in proton–proton collisions at $\sqrt{s} = 7$ and 8 TeV. JHEP **08**, 029 (2016). doi:10.1007/JHEP08(2016)029. arXiv:1603.02303
7. D0 Collaboration, Dependence of the $t\bar{t}$ production cross section on the transverse momentum of the top quark. Phys. Lett. B **693**, 515 (2010). doi:10.1016/j.physletb.2010.09.011. arXiv:1001.1900
8. CMS Collaboration, Measurement of differential top-quark-pair production cross sections in pp colisions at $\sqrt{s} = 7$ TeV. Eur. Phys. J. C **73**, 2339 (2013). doi:10.1140/epjc/s10052-013-2339-4. arXiv:1211.2220
9. CDF Collaboration, Measurement of the differential cross section $d\sigma/d(\cos\theta_t)$ for top-quark pair production in $p\bar{p}$ collisions at $\sqrt{s} = 1.96$ TeV. Phys. Rev. Lett. **111**, 182002 (2013). doi:10.1103/PhysRevLett.111.182002. arXiv:1306.2357
10. D0 Collaboration, Measurement of differential $t\bar{t}$ production cross sections in $p\bar{p}$ collisions. Phys. Rev. D **90**, 092006 (2014). doi:10.1103/PhysRevD.90.092006. arXiv:1401.5785
11. ATLAS Collaboration, Measurements of normalized differential cross sections for $t\bar{t}$ production in pp collisions at $\sqrt{s} = 7$ TeV using the ATLAS detector. Phys. Rev. D **90**, 072004 (2014). doi:10.1103/PhysRevD.90.072004. arXiv:1407.0371
12. ATLAS Collaboration, Differential top–antitop cross-section measurements as a function of observables constructed from final-state particles using pp collisions at $\sqrt{s} = 7$ TeV in the ATLAS detector. JHEP **06**, 100 (2015). doi:10.1007/JHEP06(2015)100. arXiv:1502.05923
13. CMS Collaboration, Measurement of the differential cross section for top quark pair production in pp collisions at $\sqrt{s} = 8$ TeV. Eur. Phys. J. C **75**, 542 (2015). doi:10.1140/epjc/s10052-015-3709-x. arXiv:1505.04480
14. CMS Collaboration, Measurement of the $t\bar{t}$ production cross section in the all-jets final state in pp collisions at $\sqrt{s} = 8$ TeV. Eur. Phys. J. C **76**, 128 (2016). doi:10.1140/epjc/s10052-016-3956-5. arXiv:1509.06076
15. ATLAS Collaboration, Measurement of top quark pair differential cross-sections in the dilepton channel in pp collisions at $\sqrt{s} = 7$ and 8 TeV with ATLAS. Phys. Rev. D **94**(9), 092003 (2016). doi:10.1103/PhysRevD.94.092003. arXiv:1607.07281
16. ATLAS Collaboration, Measurement of the differential cross-section of highly boosted top quarks as a function of their transverse momentum in $\sqrt{s} = 8$ TeV proton-proton collisions using the ATLAS detector. Phys. Rev. D **93**, 032009 (2016). doi:10.1103/PhysRevD.93.032009. arXiv:1510.03818
17. CMS Collaboration, Measurement of the integrated and differential $t\bar{t}$ production cross sections for high-p_T top quarks in pp collisions at $\sqrt{s} = 8$ TeV. Phys. Rev. D **94**, 072002 (2016). doi:10.1103/PhysRevD.94.072002. arXiv:1605.00116
18. CMS Collaboration, Search for anomalous $t\bar{t}$ production in the highly-boosted all-hadronic final state. JHEP **09**, 029 (2012). doi:10.1007/JHEP09(2012)029. arXiv:1204.2488
19. ATLAS Collaboration, A search for $t\bar{t}$resonances in lepton+jets events with highly boosted top quarks collected in pp collisions at $\sqrt{s} = 7$ TeV with the ATLAS detector. JHEP **09**, 041 (2012). doi:10.1007/JHEP09(2012)041. arXiv:1207.2409
20. ATLAS Collaboration, Search for resonances decaying into top-quark pairs using fully hadronic decays in pp collisions with ATLAS at $\sqrt{s} = 7$ TeV. JHEP **01**, 116 (2013). doi:10.1007/JHEP01(2013)116. arXiv:1211.2202
21. ATLAS Collaboration, Search for $t\bar{t}$ resonances in the lepton plus jets final state with ATLAS using 4.7 fb^{-1} of pp collisions at $\sqrt{s} = 7$ TeV. Phys. Rev. D **88**, 012004 (2013). doi:10.1103/PhysRevD.88.012004. arXiv:1305.2756
22. CMS Collaboration, Searches for new physics using the $t\bar{t}$ invariant mass distribution in pp collisions at $\sqrt{s} = 8$ TeV. Phys. Rev. Lett. **111**, 211804 (2013). doi:10.1103/PhysRevLett.111.

211804. arXiv: 1309.2030. **(Erratum: Phys. Rev. Lett. 112, 119903 (2014))**
23. ATLAS Collaboration, Search for $W' \to tb \to qqbb$ decays in pp collisions at $\sqrt{s}$ = 8 TeV with the ATLAS detector. Eur. Phys. J. C **75**, 165 (2015). doi:10.1140/epjc/s10052-015-3372-2. arXiv:1408.0886
24. CMS Collaboration, Search for vector-like T quarks decaying to top quarks and Higgs bosons in the all-hadronic channel using jet substructure. JHEP **06**, 080 (2015). doi:10.1007/JHEP06(2015)080. arXiv:1503.01952
25. ATLAS Collaboration, A search for $t\bar{t}$ resonances using lepton-plus-jets events in proton-proton collisions at $\sqrt{s}$ = 8 TeV with the ATLAS detector. JHEP **08**, 148 (2015). doi:10.1007/JHEP08(2015)148. arXiv:1505.07018
26. CMS Collaboration, Search for resonant $t\bar{t}$ production in proton–proton collisions at $\sqrt{s}$ = 8 TeV. Phys. Rev. D **93**, 012001 (2016). doi:10.1103/PhysRevD.93.012001. arXiv:1506.03062
27. CMS Collaboration, Search for the production of an excited bottom quark decaying to tW in proton-proton collisions at $\sqrt{s}$ = 8 TeV. JHEP **01**, 166 (2016). doi:10.1007/JHEP01(2016)166. arXiv:1509.08141
28. ATLAS Collaboration, Search for the production of single vector-like and excited quarks in the Wt final state in pp collisions at $\sqrt{s}$ = 8 TeV with the ATLAS detector. JHEP **02**, 110 (2016). doi:10.1007/JHEP02(2016)110. arXiv:1510.02664
29. ATLAS Collaboration, Jet mass and substructure of inclusive jets in $\sqrt{s}$ = 7 TeV pp collisions with the ATLAS experiment. JHEP **05**, 128 (2012). doi:10.1007/JHEP05(2012)128. arXiv:1203.4606
30. CMS Collaboration, Studies of jet mass in dijet and W/Z + jet events. JHEP **05**, 090 (2013). doi:10.1007/JHEP05(2013)090. arXiv:1303.4811
31. A.H. Hoang, I.W. Stewart, Top mass measurements from jets and the Tevatron top-quark mass. Nucl. Phys. Proc. Suppl. **185**, 220 (2008). doi:10.1016/j.nuclphysbps.2008.10.028. arXiv:0808.0222
32. CDF and D0 Collaborations, Combination of the top-quark mass measurements from the Tevatron collider. Phys. Rev. D **86**, 092003 (2012). doi:10.1103/PhysRevD.86.092003. arXiv:1207.1069
33. ATLAS Collaboration, Measurement of the top quark mass in the $t\bar{t} \to$ lepton+jets and $t\bar{t} \to$ dilepton channels using $\sqrt{s} = 7$ TeV ATLAS data. Eur. Phys. J. C **75**, 330 (2015). doi:10.1140/epjc/s10052-015-3544-0. arXiv:1503.05427
34. ATLAS Collaboration, Determination of the top-quark pole mass using tt̄+ 1-jet events collected with the ATLAS experiment in 7 TeV pp collisions. JHEP **10**, 121 (2015). doi:10.1007/JHEP10(2015)121. arXiv:1507.01769
35. CMS Collaboration, Measurement of the top quark mass using proton-proton data at $\sqrt{s} = 7$ and 8 TeV. Phys. Rev. D **93**, 072004 (2016). doi:10.1103/PhysRevD.93.072004. arXiv:1509.04044
36. CMS Collaboration, Measurement of the top quark mass using charged particles in pp collisions at $\sqrt{s}$ = 8 TeV. Phys. Rev. D **93**, 092006 (2016). doi:10.1103/PhysRevD.93.092006. arXiv:1603.06536
37. ATLAS Collaboration, Measurement of the top quark mass in the $t\bar{t} \to$ dilepton channel from $\sqrt{s}$ = 8 TeV ATLAS data. Phys. Lett. B **761**, 350 (2016). doi:10.1016/j.physletb.2016.08.042. arXiv:1606.02179
38. C.W. Bauer, S. Fleming, M.E. Luke, Summing Sudakov logarithms in $B \to X_s + \gamma$ in effective field theory. Phys. Rev. D **63**, 014006 (2000). doi:10.1103/PhysRevD.63.014006. arXiv:hep-ph/0005275
39. C.W. Bauer, S. Fleming, D. Pirjol, I.W. Stewart, An effective field theory for collinear and soft gluons: heavy to light decays. Phys. Rev. D **63**, 114020 (2001). doi:10.1103/PhysRevD.63.114020. arXiv:hep-ph/0011336
40. C.W. Bauer, I.W. Stewart, Invariant operators in collinear effective theory. Phys. Lett. B **516**, 134 (2001). doi:10.1016/S0370-2693(01)00902-9. arXiv:hep-ph/0107001
41. C.W. Bauer, D. Pirjol, I.W. Stewart, Soft-collinear factorization in effective field theory. Phys. Rev. D **65**, 054022 (2002). doi:10.1103/PhysRevD.65.054022. arXiv:hep-ph/0109045
42. S. Fleming, A.H. Hoang, S. Mantry, I.W. Stewart, Jets from massive unstable particles: top-mass determination. Phys. Rev. D **77**, 074010 (2008). doi:10.1103/PhysRevD.77.074010. arXiv:hep-ph/0703207
43. S. Fleming, A.H. Hoang, S. Mantry, I.W. Stewart, Top jets in the peak region: factorization analysis with next-to-leading-log resummation. Phys. Rev. D **77**, 114003 (2008). doi:10.1103/PhysRevD.77.114003. arXiv:0711.2079
44. A.H. Hoang, A. Pathak, P. Pietrulewicz, I.W. Stewart, Hard matching for boosted tops at two loops. JHEP **12**, 059 (2015). doi:10.1007/JHEP12(2015)059. arXiv:1508.04137
45. M. Butenschoen et al., Top quark mass calibration for Monte Carlo event generators. Phys. Rev. Lett. **117**, 232001 (2016). doi:10.1103/PhysRevLett.117.232001. arXiv:1608.01318
46. S. Moch et al., High precision fundamental constants at the TeV scale. Proceedings of the Mainz Institute for Theoretical Physics (MITP) Scientific Program on High Precision Fundamental Constants at the TeV Scale, March 10–21. 2014. arXiv:1405.4781
47. A.H. Hoang, *The top mass: interpretation and theoretical uncertainties*. 7th International Workshop on Top Quark Physics (TOP2014) Cannes, France. 2014. arXiv: 1412.3649
48. G. Corcella, Interpretation of the top-quark mass measurements: a theory overview. 8th International Workshop on Top Quark Physics (TOP2015) Ischia, Italy. 2015. arXiv: 1511.08429
49. Y.L. Dokshitzer, G.D. Leder, S. Moretti, B.R. Webber, Better jet clustering algorithms. JHEP **08**, 001 (1997). doi:10.1088/1126-6708/1997/08/001. arXiv:hep-ph/9707323
50. M. Wobisch, T. Wengler, in *Hadronization Corrections to Jet Cross Sections in Deep-Inelastic Scattering*. Monte Carlo Generators for HERA Physics (Hamburg, Germany, 1998). arXiv:hep-ph/9907280
51. CMS Collaboration, The CMS trigger system. JINST **12**, P01020 (2017). doi:10.1088/1748-0221/12/01/P01020. arXiv:1609.02366
52. CMS Collaboration, The CMS experiment at the CERN LHC. JINST **3**, S08004 (2008). doi:10.1088/1748-0221/3/08/S08004
53. CMS Collaboration, Particle-flow event reconstruction in CMS and performance for jets, taus, and $E_{\mathrm{T}}^{\mathrm{miss}}$. CMS Physics Analysis Summary CMS-PAS-PFT-09-001 (2009)
54. CMS Collaboration, Commissioning of the particle-flow event reconstruction with the first LHC collisions recorded in the CMS detector. CMS Physics Analysis Summary CMS-PAS-PFT-10-001 (2010)
55. CMS Collaboration, Description and performance of track and primary-vertex reconstruction with the CMS tracker. JINST **9**, P10009 (2014). doi:10.1088/1748-0221/9/10/P10009. arXiv:1405.6569
56. CMS Collaboration, Performance of CMS muon reconstruction in pp collision events at $\sqrt{s}$ = 7 TeV. JINST **7**, P10002 (2012). doi:10.1088/1748-0221/7/10/P10002. arXiv:1206.4071
57. CMS Collaboration, The performance of the CMS muon detector in proton-proton collisions at sqrt(s) = 7 TeV at the LHC. JINST **8**, P11002 (2013). doi:10.1088/1748-0221/8/11/P11002. arXiv:1306.6905
58. CMS Collaboration, Performance of electron reconstruction and selection with the CMS detector in proton–proton collisions at $\sqrt{s}$ = 8 TeV. JINST **10**, P06005 (2015). doi:10.1088/1748-0221/10/06/P06005. arXiv:1502.02701
59. CMS Collaboration, Energy calibration and resolution of the CMS electromagnetic calorimeter in pp collisions at $\sqrt{s}$ = 7 TeV.

JINST **8**, P09009 (2013). doi:10.1088/1748-0221/8/09/P09009. arXiv:1306.2016
60. M. Cacciari, G.P. Salam, G. Soyez, FastJet user manual. Eur. Phys. J. C **72**, 1896 (2012). doi:10.1140/epjc/s10052-012-1896-2. arXiv:1111.6097
61. M. Cacciari, G.P. Salam, G. Soyez, The anti-k_t jet clustering algorithm. JHEP **04**, 063 (2008). doi:10.1088/1126-6708/2008/04/063. arXiv:0802.1189
62. M. Cacciari, G.P. Salam, G. Soyez, The catchment area of jets. JHEP **04**, 005 (2008). doi:10.1088/1126-6708/2008/04/005. arXiv:0802.1188
63. CMS Collaboration, Determination of jet energy calibration and transverse momentum resolution in CMS. JINST **6**, P11002 (2011). doi:10.1088/1748-0221/6/11/P11002. arXiv:1107.4277
64. CMS Collaboration, Jet energy scale and resolution in the CMS experiment in pp collisions at 8 TeV. JINST (2016). arXiv:1607.03663. **(Submitted)**
65. CMS Collaboration, Identification of b-quark jets with the CMS experiment. JINST **8**, P04013 (2013). doi:10.1088/1748-0221/8/04/P04013. arXiv:1211.4462
66. CMS Collaboration, Jet performance in pp collisions at 7 tev. CMS Physics Analysis Summary CMS-PAS-JME-10-003 (2010)
67. CMS Collaboration, Missing transverse energy performance of the CMS detector. JINST **6**, P09001 (2011). doi:10.1088/1748-0221/6/09/P09001. arXiv:1106.5048
68. P. Nason, A new method for combining NLO QCD with shower Monte Carlo algorithms. JHEP **11**, 040 (2004). doi:10.1088/1126-6708/2004/11/040. arXiv:hep-ph/0409146
69. S. Frixione, P. Nason, C. Oleari, Matching NLO QCD computations with parton shower simulations: the POWHEG method. JHEP **11**, 070 (2007). doi:10.1088/1126-6708/2007/11/070. arXiv:0709.2092
70. S. Alioli, P. Nason, C. Oleari, E. Re, A general framework for implementing NLO calculations in shower Monte Carlo programs: the POWHEG BOX. JHEP **06**, 043 (2010). doi:10.1007/JHEP06(2010)043. arXiv:1002.2581
71. S. Alioli, P. Nason, C. Oleari, E. Re, NLO single-top production matched with shower in POWHEG: s- and t-channel contributions. JHEP **09**, 111 (2009). doi:10.1088/1126-6708/2009/09/111. arXiv: 0907.4076. **(Erratum: JHEP 02, 011 (2010))**
72. E. Re, Single-top Wt-channel production matched with parton showers using the POWHEG method. Eur. Phys. J. C **71**, 1547 (2011). doi:10.1140/epjc/s10052-011-1547-z. arXiv:1009.2450
73. J. Alwall et al., The automated computation of tree-level and next-to-leading order differential cross sections, and their matching to parton shower simulations. JHEP **07**, 079 (2014). doi:10.1007/JHEP07(2014)079. arXiv:1405.0301
74. P. Artoisenet, R. Frederix, O. Mattelaer, R. Rietkerk, Automatic spin-entangled decays of heavy resonances in Monte Carlo simulations. JHEP **03**, 015 (2013). doi:10.1007/JHEP03(2013)015. arXiv:1212.3460
75. T. Sjöstrand, S. Mrenna, P. Skands, PYTHIA 6.4 physics and manual. JHEP **05**, 026 (2006). doi:10.1088/1126-6708/2006/05/026. arXiv:hep-ph/0603175
76. S. Frixione, B.R. Webber, Matching NLO QCD computations and parton shower simulations. JHEP **06**, 029 (2002). doi:10.1088/1126-6708/2002/06/029. arXiv:hep-ph/0204244
77. M.L. Mangano, M. Moretti, F. Piccinini, M. Treccani, Matching matrix elements and shower evolution for top-quark production in hadronic collisions. JHEP **01**, 013 (2007). doi:10.1088/1126-6708/2007/01/013. arXiv:hep-ph/0611129
78. P.M. Nadolsky et al., Implications of CTEQ global analysis for collider observables. Phys. Rev. D **78**, 013004 (2008). doi:10.1103/PhysRevD.78.013004. arXiv:0802.0007
79. H.-L. Lai et al., New parton distributions for collider physics. Phys. Rev. D **82**, 074024 (2010). doi:10.1103/PhysRevD.82.074024. arXiv:1007.2241
80. J. Pumplin et al., New generation of parton distributions with uncertainties from global QCD analysis. JHEP **07**, 012 (2002). doi:10.1088/1126-6708/2002/07/012. arXiv:hep-ph/0201195
81. CMS Collaboration, Study of the underlying event at forward rapidity in pp collisions at $\sqrt{s}$ = 0.9, 2.76, and 7 TeV. JHEP **04**, 072 (2013). doi:10.1007/JHEP04(2013)072. arXiv:1302.2394
82. CMS Collaboration, Event generator tunes obtained from underlying event and multiparton scattering measurements. Eur. Phys. J. C **76**, 155 (2016). doi:10.1140/epjc/s10052-016-3988-x. arXiv:1512.00815
83. G. Corcella et al., HERWIG 6: an event generator for hadron emission reactions with interfering gluons (including supersymmetric processes). JHEP **01**, 010 (2001). doi:10.1088/1126-6708/2001/01/010. arXiv:hep-ph/0011363
84. N. Kidonakis, NNLL threshold resummation for top-pair and single-top production. Phys. Part. Nucl. **45**, 714 (2014). doi:10.1134/S1063779614040091. arXiv:1210.7813
85. R. Gavin, Y. Li, F. Petriello, S. Quackenbush, FEWZ 2.0: A code for hadronic Z production at next-to-next-to-leading order. Comput. Phys. Commun. **182**, 2388 (2011). doi:10.1016/j.cpc.2011.06.008. arXiv:1011.3540
86. R. Gavin, Y. Li, F. Petriello, S. Quackenbush, W physics at the LHC with FEWZ 2.1. Comput. Phys. Commun. **184**, 208 (2013). doi:10.1016/j.cpc.2012.09.005. arXiv:1201.5896
87. Y. Li, F. Petriello, Combining QCD and electroweak corrections to dilepton production in the framework of the FEWZ simulation code. Phys. Rev. D **86**, 094034 (2012). doi:10.1103/PhysRevD.86.094034. arXiv:1208.5967
88. J.M. Campbell, R.K. Ellis, K. Williams, Vector boson pair production at the LHC. JHEP **07**, 018 (2011). doi:10.1007/JHEP07(2011)018. arXiv:1105.0020
89. M. Beneke, P. Falgari, S. Klein, C. Schwinn, Hadronic top-quark pair production with NNLL threshold resummation. Nucl. Phys. B **855**, 695 (2012). doi:10.1016/j.nuclphysb.2011.10.021. arXiv:1109.1536
90. M. Cacciari et al., Top-pair production at hadron colliders with next-to-next-to-leading logarithmic soft-gluon resummation. Phys. Lett. B **710**, 612 (2012). doi:10.1016/j.physletb.2012.03.013. arXiv:1111.5869
91. P. Bärnreuther, M. Czakon, A. Mitov, Percent-level-precision physics at the tevatron: next-to-leading order QCD corrections to $q\bar{q} \to t\bar{t} + X$. Phys. Rev. Lett. **109**, 132001 (2012). doi:10.1103/PhysRevLett.109.132001. arXiv:1204.5201
92. M. Czakon, A. Mitov, NNLO corrections to top-pair production at hadron colliders: the all-fermionic scattering channels. JHEP **12**, 054 (2012). doi:10.1007/JHEP12(2012)054. arXiv:1207.0236
93. M. Czakon, A. Mitov, NNLO corrections to top pair production at hadron colliders: the quark–gluon reaction. JHEP **01**, 080 (2013). doi:10.1007/JHEP01(2013)080. arXiv:1210.6832
94. M. Czakon, P. Fiedler, A. Mitov, Total top-quark pair-production cross section at hadron colliders through $O(\alpha_S^4)$. Phys. Rev. Lett. **110**, 252004 (2013). doi:10.1103/PhysRevLett.110.252004. arXiv:1303.6254
95. M. Czakon, A. Mitov, Top++: a program for the calculation of the top-pair cross-section at hadron colliders. Comput. Phys. Commun. **185**, 2930 (2014). doi:10.1016/j.cpc.2014.06.021. arXiv:1112.5675
96. GEANT4 Collaboration, GEANT4—a simulation toolkit. Nucl. Instrum. Meth. A **506**, 250 (2003). doi:10.1016/S0168-9002(03)01368-8

97. CMS Collaboration, Performance of the CMS missing transverse momentum reconstruction in pp data at $\sqrt{s} = 8$ TeV. JINST **10**, P02006 (2015). doi:10.1088/1748-0221/10/02/P02006. arXiv:1411.0511
98. J. Thaler, K. Van Tilburg, Identifying boosted objects with N-subjettiness. JHEP **03**, 015 (2011). doi:10.1007/JHEP03(2011)015. arXiv:1011.2268
99. J. Thaler, K. Van Tilburg, Maximizing boosted top identification by minimizing N-subjettiness. JHEP **02**, 093 (2012). doi:10.1007/JHEP02(2012)093. arXiv:1108.2701
100. D.E. Kaplan, K. Rehermann, M.D. Schwartz, B. Tweedie, Top tagging: a method for identifying boosted hadronically decaying top quarks. Phys. Rev. Lett. **101**, 142001 (2008). doi:10.1103/PhysRevLett.101.142001. arXiv:0806.0848
101. CMS Collaboration, A Cambridge-Aachen (C-A) based jet algorithm for boosted top-jet tagging. CMS Physics Analysis Summary CMS-PAS-JME-09-001 (2009)
102. T. Plehn, G.P. Salam, M. Spannowsky, Fat jets for a light Higgs boson. Phys. Rev. Lett. **104**, 111801 (2010). doi:10.1103/PhysRevLett.104.111801. arXiv:0910.5472
103. T. Plehn, M. Spannowsky, M. Takeuchi, D. Zerwas, Stop reconstruction with tagged tops. JHEP **10**, 078 (2010). doi:10.1007/JHEP10(2010)078. arXiv:1006.2833
104. T. Lapsien, R. Kogler, J. Haller, A new tagger for hadronically decaying heavy particles at the LHC. Eur. Phys. J. C **76**, 600 (2016). doi:10.1140/epjc/s10052-016-4443-8. arXiv:1606.04961
105. Y.-T. Chien, R. Kelley, M.D. Schwartz, H.X. Zhu, Resummation of jet mass at hadron colliders. Phys. Rev. D **87**, 014010 (2013). doi:10.1103/PhysRevD.87.014010. arXiv:1208.0010
106. M. Dasgupta, G.P. Salam, Resummation of non-global QCD observables. Phys. Lett. B **512**, 323 (2001). doi:10.1016/S0370-2693(01)00725-0. arXiv:hep-ph/0104277
107. S. Schmitt, TUnfold: an algorithm for correcting migration effects in high energy physics. JINST **7**, T10003 (2012). doi:10.1088/1748-0221/7/10/T10003. arXiv:1205.6201
108. S. Schmitt, in *Data Unfolding Methods in High Energy Physics*. 12th Conference on Quark Confinement and the Hadron Spectrum (Confinement XII) (Thessaloniki, Greece, 2016). arXiv:1611.01927
109. G. Antchev et al., First measurement of the total proton-proton cross section at the LHC energy of $\sqrt{s} = 7$ TeV. Europhys. Lett. **96**, 21002 (2011). doi:10.1209/0295-5075/96/21002. arXiv:1110.1395
110. CMS Collaboration, Measurement of the production cross section of the W boson in association with two b jets in pp collisions at $\sqrt{s} = 8$ TeV. EPJC (2016). arXiv: 1608.07561. **(Submitted)**
111. CMS Collaboration, Observation of the associated production of a single top quark and a W boson in pp collisions at $\sqrt{s} = 8$ TeV. Phys. Rev. Lett. **112**, 231802 (2014). doi:10.1103/PhysRevLett.112.231802. arXiv:1401.2942
112. CMS Collaboration, CMS luminosity based on pixel cluster counting—summer 2013 update. CMS Physics Analysis Summary CMS-PAS-LUM-13-001 (2013)
113. M. Czakon, D. Heymes, A. Mitov, High-precision differential predictions for top-quark pairs at the LHC. Phys. Rev. Lett. **116**, 082003 (2016). doi:10.1103/PhysRevLett.116.082003. arXiv:1511.00549
114. ATLAS Collaboration, Measurement of the $\mathrm{t\bar{t}}$ production cross-section using $\mathrm{e}\mu$ events with b-tagged jets in pp collisions at $\sqrt{s} =$ 7 and 8 TeV with the ATLAS detector. Eur. Phys. J. C **74**, 3109 (2014). doi:10.1140/epjc/s10052-014-3109-7. arXiv:1406.5375
115. Gfitter Group, The global electroweak fit at NNLO and prospects for the LHC and ILC. Eur. Phys. J. C **74**, 3046 (2014). doi:10.1140/epjc/s10052-014-3046-5. arXiv:1407.3792
116. ATLAS, CDF, CMS and D0 Collaborations, First combination of tevatron and LHC measurements of the top-quark mass (2014). arXiv:1403.4427

CMS Collaboration

Yerevan Physics Institute, Yerevan, Armenia
A. M. Sirunyan, A. Tumasyan

Institut für Hochenergiephysik, Wien, Austria
W. Adam, E. Asilar, T. Bergauer, J. Brandstetter, E. Brondolin, M. Dragicevic, J. Erö, M. Flechl, M. Friedl, R. Frühwirth[1], V. M. Ghete, C. Hartl, N. Hörmann, J. Hrubec, M. Jeitler[1], A. König, I. Krätschmer, D. Liko, T. Matsushita, I. Mikulec, D. Rabady, N. Rad, B. Rahbaran, H. Rohringer, J. Schieck[1], J. Strauss, W. Waltenberger, C.-E. Wulz[1]

Institute for Nuclear Problems, Minsk, Belarus
O. Dvornikov, V. Makarenko, V. Mossolov, J. Suarez Gonzalez, V. Zykunov

National Centre for Particle and High Energy Physics, Minsk, Belarus
N. Shumeiko

Universiteit Antwerpen, Antwerpen, Belgium
S. Alderweireldt, E. A. De Wolf, X. Janssen, J. Lauwers, M. Van De Klundert, H. Van Haevermaet, P. Van Mechelen, N. Van Remortel, A. Van Spilbeeck

Vrije Universiteit Brussel, Brussel, Belgium
S. Abu Zeid, F. Blekman, J. D'Hondt, N. Daci, I. De Bruyn, K. Deroover, S. Lowette, S. Moortgat, L. Moreels, A. Olbrechts, Q. Python, K. Skovpen, S. Tavernier, W. Van Doninck, P. Van Mulders, I. Van Parijs

Université Libre de Bruxelles, Bruxelles, Belgium
H. Brun, B. Clerbaux, G. De Lentdecker, H. Delannoy, G. Fasanella, L. Favart, R. Goldouzian, A. Grebenyuk,

G. Karapostoli, T. Lenzi, A. Léonard, J. Luetic, T. Maerschalk, A. Marinov, A. Randle-conde, T. Seva, C. Vander Velde, P. Vanlaer, D. Vannerom, R. Yonamine, F. Zenoni, F. Zhang[2]

Ghent University, Ghent, Belgium
A. Cimmino, T. Cornelis, D. Dobur, A. Fagot, M. Gul, I. Khvastunov, D. Poyraz, S. Salva, R. Schöfbeck, M. Tytgat, W. Van Driessche, E. Yazgan, N. Zaganidis

Université Catholique de Louvain, Louvain-la-Neuve, Belgium
H. Bakhshiansohi, C. Beluffi[3], O. Bondu, S. Brochet, G. Bruno, A. Caudron, S. De Visscher, C. Delaere, M. Delcourt, B. Francois, A. Giammanco, A. Jafari, M. Komm, G. Krintiras, V. Lemaitre, A. Magitteri, A. Mertens, M. Musich, K. Piotrzkowski, L. Quertenmont, M. Selvaggi, M. Vidal Marono, S. Wertz

Université de Mons, Mons, Belgium
N. Beliy

Centro Brasileiro de Pesquisas Fisicas, Rio de Janeiro, Brazil
W. L. Aldá Júnior, F. L. Alves, G. A. Alves, L. Brito, C. Hensel, A. Moraes, M. E. Pol, P. Rebello Teles

Universidade do Estado do Rio de Janeiro, Rio de Janeiro, Brazil
E. Belchior Batista Das Chagas, W. Carvalho, J. Chinellato[4], A. Custódio, E. M. Da Costa, G. G. Da Silveira[5], D. De Jesus Damiao, C. De Oliveira Martins, S. Fonseca De Souza, L. M. Huertas Guativa, H. Malbouisson, D. Matos Figueiredo, C. Mora Herrera, L. Mundim, H. Nogima, W. L. Prado Da Silva, A. Santoro, A. Sznajder, E. J. Tonelli Manganote[4], F. Torres Da Silva De Araujo, A. Vilela Pereira

Universidade Estadual Paulista[a], Universidade Federal do ABC[b], São Paulo, Brazil
S. Ahuja[a], C. A. Bernardes[a], S. Dogra[a], T. R. Fernandez Perez Tomei[a], E. M. Gregores[b], P. G. Mercadante[b], C. S. Moon[a], S. F. Novaes[a], Sandra S. Padula[a], D. Romero Abad[b], J. C. Ruiz Vargas[a]

Institute for Nuclear Research and Nuclear Energy, Sofia, Bulgaria
A. Aleksandrov, R. Hadjiiska, P. Iaydjiev, M. Rodozov, S. Stoykova, G. Sultanov, M. Vutova

University of Sofia, Sofia, Bulgaria
A. Dimitrov, I. Glushkov, L. Litov, B. Pavlov, P. Petkov

Beihang University, Beijing, China
W. Fang[6]

Institute of High Energy Physics, Beijing, China
M. Ahmad, J. G. Bian, G. M. Chen, H. S. Chen, M. Chen, Y. Chen[7], T. Cheng, C. H. Jiang, D. Leggat, Z. Liu, F. Romeo, M. Ruan, S. M. Shaheen, A. Spiezia, J. Tao, C. Wang, Z. Wang, H. Zhang, J. Zhao

State Key Laboratory of Nuclear Physics and Technology, Peking University, Beijing, China
Y. Ban, G. Chen, Q. Li, S. Liu, Y. Mao, S. J. Qian, D. Wang, Z. Xu

Universidad de Los Andes, Bogota, Colombia
C. Avila, A. Cabrera, L. F. Chaparro Sierra, C. Florez, J. P. Gomez, C. F. González Hernández, J. D. Ruiz Alvarez, J. C. Sanabria

University of Split, Faculty of Electrical Engineering, Mechanical Engineering and Naval Architecture, Split, Croatia
N. Godinovic, D. Lelas, I. Puljak, P. M. Ribeiro Cipriano, T. Sculac

University of Split, Faculty of Science, Split, Croatia
Z. Antunovic, M. Kovac

Institute Rudjer Boskovic, Zagreb, Croatia
V. Brigljevic, D. Ferencek, K. Kadija, B. Mesic, T. Susa

University of Cyprus, Nicosia, Cyprus
A. Attikis, G. Mavromanolakis, J. Mousa, C. Nicolaou, F. Ptochos, P. A. Razis, H. Rykaczewski, D. Tsiakkouri

Charles University, Prague, Czech Republic
M. Finger[8], M. Finger Jr.[8]

Universidad San Francisco de Quito, Quito, Ecuador
E. Carrera Jarrin

Academy of Scientific Research and Technology of the Arab Republic of Egypt, Egyptian Network of High Energy Physics, Cairo, Egypt
A. A. Abdelalim[9,10], Y. Mohammed[11], E. Salama[12,13]

National Institute of Chemical Physics and Biophysics, Tallinn, Estonia
M. Kadastik, L. Perrini, M. Raidal, A. Tiko, C. Veelken

Department of Physics, University of Helsinki, Helsinki, Finland
P. Eerola, J. Pekkanen, M. Voutilainen

Helsinki Institute of Physics, Helsinki, Finland
J. Härkönen, T. Järvinen, V. Karimäki, R. Kinnunen, T. Lampén, K. Lassila-Perini, S. Lehti, T. Lindén, P. Luukka, J. Tuominiemi, E. Tuovinen, L. Wendland

Lappeenranta University of Technology, Lappeenranta, Finland
J. Talvitie, T. Tuuva

IRFU, CEA, Université Paris-Saclay, Gif-sur-Yvette, France
M. Besancon, F. Couderc, M. Dejardin, D. Denegri, B. Fabbro, J. L. Faure, C. Favaro, F. Ferri, S. Ganjour, S. Ghosh, A. Givernaud, P. Gras, G. Hamel de Monchenault, P. Jarry, I. Kucher, E. Locci, M. Machet, J. Malcles, J. Rander, A. Rosowsky, M. Titov

Laboratoire Leprince-Ringuet, Ecole Polytechnique, IN2P3-CNRS, Palaiseau, France
A. Abdulsalam, I. Antropov, S. Baffioni, F. Beaudette, P. Busson, L. Cadamuro, E. Chapon, C. Charlot, O. Davignon, R. Granier de Cassagnac, M. Jo, S. Lisniak, P. Miné, M. Nguyen, C. Ochando, G. Ortona, P. Paganini, P. Pigard, S. Regnard, R. Salerno, Y. Sirois, A. G. Stahl Leiton, T. Strebler, Y. Yilmaz, A. Zabi, A. Zghiche

Institut Pluridisciplinaire Hubert Curien (IPHC), Université de Strasbourg, CNRS-IN2P3, Strasbourg, France
J.-L. Agram[14], J. Andrea, A. Aubin, D. Bloch, J.-M. Brom, M. Buttignol, E. C. Chabert, N. Chanon, C. Collard, E. Conte[14], X. Coubez, J.-C. Fontaine[14], D. Gelé, U. Goerlach, A.-C. Le Bihan, P. Van Hove

Centre de Calcul de l'Institut National de Physique Nucleaire et de Physique des Particules CNRS/IN2P3, Villeurbanne, France
S. Gadrat

Université de Lyon, Université Claude Bernard Lyon 1, CNRS-IN2P3, Institut de Physique Nucléaire de Lyon, Villeurbanne, France
S. Beauceron, C. Bernet, G. Boudoul, C. A. Carrillo Montoya, R. Chierici, D. Contardo, B. Courbon, P. Depasse, H. El Mamouni, J. Fay, S. Gascon, M. Gouzevitch, G. Grenier, B. Ille, F. Lagarde, I. B. Laktineh, M. Lethuillier, L. Mirabito, A. L. Pequegnot, S. Perries, A. Popov[15], D. Sabes, V. Sordini, M. Vander Donckt, P. Verdier, S. Viret

Georgian Technical University, Tbilisi, Georgia
A. Khvedelidze[8]

Tbilisi State University, Tbilisi, Georgia
Z. Tsamalaidze[8]

RWTH Aachen University, I. Physikalisches Institut, Aachen, Germany
C. Autermann, S. Beranek, L. Feld, M. K. Kiesel, K. Klein, M. Lipinski, M. Preuten, C. Schomakers, J. Schulz, T. Verlage

RWTH Aachen University, III. Physikalisches Institut A, Aachen, Germany
A. Albert, M. Brodski, E. Dietz-Laursonn, D. Duchardt, M. Endres, M. Erdmann, S. Erdweg, T. Esch, R. Fischer, A. Güth, M. Hamer, T. Hebbeker, C. Heidemann, K. Hoepfner, S. Knutzen, M. Merschmeyer, A. Meyer, P. Millet, S. Mukherjee, M. Olschewski, K. Padeken, T. Pook, M. Radziej, H. Reithler, M. Rieger, F. Scheuch, L. Sonnenschein, D. Teyssier, S. Thüer

RWTH Aachen University, III. Physikalisches Institut B, Aachen, Germany
V. Cherepanov, G. Flügge, B. Kargoll, T. Kress, A. Künsken, J. Lingemann, T. Müller, A. Nehrkorn, A. Nowack, C. Pistone, O. Pooth, A. Stahl[16]

Deutsches Elektronen-Synchrotron, Hamburg, Germany
M. Aldaya Martin, T. Arndt, C. Asawatangtrakuldee, K. Beernaert, O. Behnke, U. Behrens, A. A. Bin Anuar, K. Borras[17], A. Campbell, P. Connor, C. Contreras-Campana, F. Costanza, C. Diez Pardos, G. Dolinska, G. Eckerlin, D. Eckstein, T. Eichhorn, E. Eren, E. Gallo[18], J. Garay Garcia, A. Geiser, A. Gizhko, J. M. Grados Luyando, A. Grohsjean, P. Gunnellini, A. Harb, J. Hauk, M. Hempel[19], H. Jung, A. Kalogeropoulos, O. Karacheban[19], M. Kasemann, J. Keaveney, C. Kleinwort, I. Korol, D. Krücker, W. Lange, A. Lelek, T. Lenz, J. Leonard, K. Lipka, A. Lobanov, W. Lohmann[19], R. Mankel, I.-A. Melzer-Pellmann, A. B. Meyer, G. Mittag, J. Mnich, A. Mussgiller, D. Pitzl, R. Placakyte, A. Raspereza, B. Roland, M. Ö. Sahin, P. Saxena, T. Schoerner-Sadenius, S. Spannagel, N. Stefaniuk, G. P. Van Onsem, R. Walsh, C. Wissing

University of Hamburg, Hamburg, Germany
V. Blobel, M. Centis Vignali, A. R. Draeger, T. Dreyer, E. Garutti, D. Gonzalez, J. Haller, M. Hoffmann, A. Junkes, R. Klanner, R. Kogler, N. Kovalchuk, T. Lapsien, I. Marchesini, D. Marconi, M. Meyer, M. Niedziela, D. Nowatschin, F. Pantaleo[16], T. Peiffer, A. Perieanu, C. Scharf, P. Schleper, A. Schmidt, S. Schumann, J. Schwandt, H. Stadie, G. Steinbrück, F. M. Stober, M. Stöver, H. Tholen, D. Troendle, E. Usai, L. Vanelderen, A. Vanhoefer, B. Vormwald

Institut für Experimentelle Kernphysik, Karlsruhe, Germany
M. Akbiyik, C. Barth, S. Baur, C. Baus, J. Berger, E. Butz, R. Caspart, T. Chwalek, F. Colombo, W. De Boer, A. Dierlamm, S. Fink, B. Freund, R. Friese, M. Giffels, A. Gilbert, P. Goldenzweig, D. Haitz, F. Hartmann[16], S. M. Heindl, U. Husemann, I. Katkov[15], S. Kudella, H. Mildner, M. U. Mozer, Th. Müller, M. Plagge, G. Quast, K. Rabbertz, S. Röcker, F. Roscher, M. Schröder, I. Shvetsov, G. Sieber, H. J. Simonis, R. Ulrich, S. Wayand, M. Weber, T. Weiler, S. Williamson, C. Wöhrmann, R. Wolf

Institute of Nuclear and Particle Physics (INPP), NCSR Demokritos, Aghia Paraskevi, Greece
G. Anagnostou, G. Daskalakis, T. Geralis, V. A. Giakoumopoulou, A. Kyriakis, D. Loukas, I. Topsis-Giotis

National and Kapodistrian University of Athens, Athens, Greece
S. Kesisoglou, A. Panagiotou, N. Saoulidou, E. Tziaferi

University of Ioánnina, Ioánnina, Greece
I. Evangelou, G. Flouris, C. Foudas, P. Kokkas, N. Loukas, N. Manthos, I. Papadopoulos, E. Paradas

MTA-ELTE Lendület CMS Particle and Nuclear Physics Group, Eötvös Loránd University, Budapest, Hungary
N. Filipovic, G. Pasztor

Wigner Research Centre for Physics, Budapest, Hungary
G. Bencze, C. Hajdu, D. Horvath[20], F. Sikler, V. Veszpremi, G. Vesztergombi[21], A. J. Zsigmond

Institute of Nuclear Research ATOMKI, Debrecen, Hungary
N. Beni, S. Czellar, J. Karancsi[22], A. Makovec, J. Molnar, Z. Szillasi

Institute of Physics, University of Debrecen, Debrecen, Hungary
M. Bartók[21], P. Raics, Z. L. Trocsanyi, B. Ujvari

Indian Institute of Science (IISc), Bangalore, India
J. R. Komaragiri

National Institute of Science Education and Research, Bhubaneswar, India
S. Bahinipati[23], S. Bhowmik[24], S. Choudhury[25], P. Mal, K. Mandal, A. Nayak[26], D. K. Sahoo[23], N. Sahoo, S. K. Swain

Panjab University, Chandigarh, India
S. Bansal, S. B. Beri, V. Bhatnagar, R. Chawla, U. Bhawandeep, A. K. Kalsi, A. Kaur, M. Kaur, R. Kumar, P. Kumari, A. Mehta, M. Mittal, J. B. Singh, G. Walia

University of Delhi, Delhi, India
Ashok Kumar, A. Bhardwaj, B. C. Choudhary, R. B. Garg, S. Keshri, S. Malhotra, M. Naimuddin, K. Ranjan, R. Sharma, V. Sharma

Saha Institute of Nuclear Physics, Kolkata, India
R. Bhattacharya, S. Bhattacharya, K. Chatterjee, S. Dey, S. Dutt, S. Dutta, S. Ghosh, N. Majumdar, A. Modak, K. Mondal, S. Mukhopadhyay, S. Nandan, A. Purohit, A. Roy, D. Roy, S. Roy Chowdhury, S. Sarkar, M. Sharan, S. Thakur

Indian Institute of Technology Madras, Madras, India
P. K. Behera

Bhabha Atomic Research Centre, Mumbai, India
R. Chudasama, D. Dutta, V. Jha, V. Kumar, A. K. Mohanty[16], P. K. Netrakanti, L. M. Pant, P. Shukla, A. Topkar

Tata Institute of Fundamental Research-A, Mumbai, India
T. Aziz, S. Dugad, G. Kole, B. Mahakud, S. Mitra, G. B. Mohanty, B. Parida, N. Sur, B. Sutar

Tata Institute of Fundamental Research-B, Mumbai, India
S. Banerjee, R. K. Dewanjee, S. Ganguly, M. Guchait, Sa. Jain, S. Kumar, M. Maity[24], G. Majumder, K. Mazumdar, T. Sarkar[24], N. Wickramage[27]

Indian Institute of Science Education and Research (IISER), Pune, India
S. Chauhan, S. Dube, V. Hegde, A. Kapoor, K. Kothekar, S. Pandey, A. Rane, S. Sharma

Institute for Research in Fundamental Sciences (IPM), Tehran, Iran
S. Chenarani[28], E. Eskandari Tadavani, S. M. Etesami[28], M. Khakzad, M. Mohammadi Najafabadi, M. Naseri, S. Paktinat Mehdiabadi[29], F. Rezaei Hosseinabadi, B. Safarzadeh[30], M. Zeinali

University College Dublin, Dublin, Ireland
M. Felcini, M. Grunewald

INFN Sezione di Bari[a], Università di Bari[b], Politecnico di Bari[c], Bari, Italy
M. Abbrescia[a,b], C. Calabria[a,b], C. Caputo[a,b], A. Colaleo[a], D. Creanza[a,c], L. Cristella[a,b], N. De Filippis[a,c], M. De Palma[a,b], L. Fiore[a], G. Iaselli[a,c], G. Maggi[a,c], M. Maggi[a], G. Miniello[a,b], S. My[a,b], S. Nuzzo[a,b], A. Pompili[a,b], G. Pugliese[a,c], R. Radogna[a,b], A. Ranieri[a], G. Selvaggi[a,b], A. Sharma[a], L. Silvestris[a,16], R. Venditti[a,b], P. Verwilligen[a]

INFN Sezione di Bologna[a], Università di Bologna[b], Bologna, Italy
G. Abbiendi[a], C. Battilana, D. Bonacorsi[a,b], S. Braibant-Giacomelli[a,b], L. Brigliadori[a,b], R. Campanini[a,b], P. Capiluppi[a,b], A. Castro[a,b], F. R. Cavallo[a], S. S. Chhibra[a,b], G. Codispoti[a,b], M. Cuffiani[a,b], G. M. Dallavalle[a], F. Fabbri[a], A. Fanfani[a,b], D. Fasanella[a,b], P. Giacomelli[a], C. Grandi[a], L. Guiducci[a,b], S. Marcellini[a], G. Masetti[a], A. Montanari[a], F. L. Navarria[a,b], A. Perrotta[a], A. M. Rossi[a,b], T. Rovelli[a,b], G. P. Siroli[a,b], N. Tosi[a,b,16]

INFN Sezione di Catania[a], Università di Catania[b], Catania, Italy
S. Albergo[a,b], S. Costa[a,b], A. Di Mattia[a], F. Giordano[a,b], R. Potenza[a,b], A. Tricomi[a,b], C. Tuve[a,b]

INFN Sezione di Firenze[a], Università di Firenze[b], Firenze, Italy
G. Barbagli[a], V. Ciulli[a,b], C. Civinini[a], R. D'Alessandro[a,b], E. Focardi[a,b], P. Lenzi[a,b], M. Meschini[a], S. Paoletti[a], L. Russo[a,31], G. Sguazzoni[a], D. Strom[a], L. Viliani[a,b,16]

INFN Laboratori Nazionali di Frascati, Frascati, Italy
L. Benussi, S. Bianco, F. Fabbri, D. Piccolo, F. Primavera[16]

INFN Sezione di Genova[a], Università di Genova[b], Genoa, Italy
V. Calvelli[a,b], F. Ferro[a], M. R. Monge[a,b], E. Robutti[a], S. Tosi[a,b]

INFN Sezione di Milano-Bicocca[a], Università di Milano-Bicocca[b], Milan, Italy
L. Brianza[a,b,16], F. Brivio[a,b], V. Ciriolo, M. E. Dinardo[a,b], S. Fiorendi[a,b,16], S. Gennai[a], A. Ghezzi[a,b], P. Govoni[a,b], M. Malberti[a,b], S. Malvezzi[a], R. A. Manzoni[a,b], D. Menasce[a], L. Moroni[a], M. Paganoni[a,b], D. Pedrini[a], S. Pigazzini[a,b], S. Ragazzi[a,b], T. Tabarelli de Fatis[a,b]

INFN Sezione di Napoli[a], Università di Napoli 'Federico II'[b], Naples, Italy, Università della Basilicata[c], Potenza, Italy, Università G. Marconi[d], Rome, Italy
S. Buontempo[a], N. Cavallo[a,c], G. De Nardo, S. Di Guida[a,d,16], M. Esposito[a,b], F. Fabozzi[a,c], F. Fienga[a,b], A. O. M. Iorio[a,b], G. Lanza[a], L. Lista[a], S. Meola[a,d,16], P. Paolucci[a,16], C. Sciacca[a,b], F. Thyssen[a]

INFN Sezione di Padova[a], Università di Padova[b], Padua, Italy, Università di Trento[c], Trento, Italy
P. Azzi[a,16], N. Bacchetta[a], L. Benato[a,b], D. Bisello[a,b], A. Boletti[a,b], R. Carlin[a,b], A. Carvalho Antunes de Oliveira[a,b], P. Checchia[a], M. Dall'Osso[a,b], P. De Castro Manzano[a], T. Dorigo[a], U. Dosselli[a], F. Gasparini[a,b], U. Gasparini[a,b], A. Gozzelino[a], S. Lacaprara[a], M. Margoni[a,b], A. T. Meneguzzo[a,b], J. Pazzini[a,b], N. Pozzobon[a,b], P. Ronchese[a,b], F. Simonetto[a,b], E. Torassa[a], M. Zanetti[a,b], P. Zotto[a,b], G. Zumerle[a,b]

INFN Sezione di Pavia[a], Università di Pavia[b], Pavia, Italy
A. Braghieri[a], F. Fallavollita[a,b], A. Magnani[a,b], P. Montagna[a,b], S. P. Ratti[a,b], V. Re[a], C. Riccardi[a,b], P. Salvini[a], I. Vai[a,b], P. Vitulo[a,b]

INFN Sezione di Perugia[a], Università di Perugia[b], Perugia, Italy
L. Alunni Solestizi[a,b], G. M. Bilei[a], D. Ciangottini[a,b], L. Fanò[a,b], P. Lariccia[a,b], R. Leonardi[a,b], G. Mantovani[a,b], M. Menichelli[a], A. Saha[a], A. Santocchia[a,b]

INFN Sezione di Pisa[a], Università di Pisa[b], Scuola Normale Superiore di Pisa[c], Pisa, Italy
K. Androsov[a,31], P. Azzurri[a,16], G. Bagliesi[a], J. Bernardini[a], T. Boccali[a], R. Castaldi[a], M. A. Ciocci[a,31], R. Dell'Orso[a], S. Donato[a,c], G. Fedi, A. Giassi[a], M. T. Grippo[a,31], F. Ligabue[a,c], T. Lomtadze[a], L. Martini[a,b], A. Messineo[a,b], F. Palla[a], A. Rizzi[a,b], A. Savoy-Navarro[a,32], P. Spagnolo[a], R. Tenchini[a], G. Tonelli[a,b], A. Venturi[a], P. G. Verdini[a]

INFN Sezione di Roma[a], Università di Roma[b], Rome, Italy
L. Barone[a,b], F. Cavallari[a], M. Cipriani[a,b], D. Del Re[a,b,16], M. Diemoz[a], S. Gelli[a,b], E. Longo[a,b], F. Margaroli[a,b], B. Marzocchi[a,b], P. Meridiani[a], G. Organtini[a,b], R. Paramatti[a], F. Preiato[a,b], S. Rahatlou[a,b], C. Rovelli[a], F. Santanastasio[a,b]

INFN Sezione di Torino[a], Università di Torino[b], Turin, Italy, Università del Piemonte Orientale[c], Novara, Italy
N. Amapane[a,b], R. Arcidiacono[a,c,16], S. Argiro[a,b], M. Arneodo[a,c], N. Bartosik[a], R. Bellan[a,b], C. Biino[a], N. Cartiglia[a], F. Cenna[a,b], M. Costa[a,b], R. Covarelli[a,b], A. Degano[a,b], N. Demaria[a], L. Finco[a,b], B. Kiani[a,b], C. Mariotti[a], S. Maselli[a], E. Migliore[a,b], V. Monaco[a,b], E. Monteil[a,b], M. Monteno[a], M. M. Obertino[a,b], L. Pacher[a,b], N. Pastrone[a], M. Pelliccioni[a], G. L. Pinna Angioni[a,b], F. Ravera[a,b], A. Romero[a,b], M. Ruspa[a,c], R. Sacchi[a,b], K. Shchelina[a,b], V. Sola[a], A. Solano[a,b], A. Staiano[a], P. Traczyk[a,b]

INFN Sezione di Trieste[a], Università di Trieste[b], Trieste, Italy
S. Belforte[a], M. Casarsa[a], F. Cossutti[a], G. Della Ricca[a,b], A. Zanetti[a]

Kyungpook National University, Taegu, Korea
D. H. Kim, G. N. Kim, M. S. Kim, S. Lee, S. W. Lee, Y. D. Oh, S. Sekmen, D. C. Son, Y. C. Yang

Chonbuk National University, Chonju, Korea
A. Lee

Chonnam National University Institute for Universe and Elementary Particles, Kwangju, Korea
H. Kim

Hanyang University, Seoul, Korea
J. A. Brochero Cifuentes, T. J. Kim

Korea University, Seoul, Korea
S. Cho, S. Choi, Y. Go, D. Gyun, S. Ha, B. Hong, Y. Jo, Y. Kim, K. Lee, K. S. Lee, S. Lee, J. Lim, S. K. Park, Y. Roh

Seoul National University, Seoul, Korea
J. Almond, J. Kim, H. Lee, S. B. Oh, B. C. Radburn-Smith, S. h. Seo, U. K. Yang, H. D. Yoo, G. B. Yu

University of Seoul, Seoul, Korea
M. Choi, H. Kim, J. H. Kim, J. S. H. Lee, I. C. Park, G. Ryu, M. S. Ryu

Sungkyunkwan University, Suwon, Korea
Y. Choi, J. Goh, C. Hwang, J. Lee, I. Yu

Vilnius University, Vilnius, Lithuania
V. Dudenas, A. Juodagalvis, J. Vaitkus

National Centre for Particle Physics, Universiti Malaya, Kuala Lumpur, Malaysia
I. Ahmed, Z. A. Ibrahim, M. A. B. Md Ali[33], F. Mohamad Idris[34], W. A. T. Wan Abdullah, M. N. Yusli, Z. Zolkapli

Centro de Investigacion y de Estudios Avanzados del IPN, Mexico City, Mexico
H. Castilla-Valdez, E. De La Cruz-Burelo, I. Heredia-De La Cruz[35], A. Hernandez-Almada, R. Lopez-Fernandez, R. Magaña Villalba, J. Mejia Guisao, A. Sanchez-Hernandez

Universidad Iberoamericana, Mexico City, Mexico
S. Carrillo Moreno, C. Oropeza Barrera, F. Vazquez Valencia

Benemerita Universidad Autonoma de Puebla, Puebla, Mexico
S. Carpinteyro, I. Pedraza, H. A. Salazar Ibarguen, C. Uribe Estrada

Universidad Autónoma de San Luis Potosí, San Luis Potosí, Mexico
A. Morelos Pineda

University of Auckland, Auckland, New Zealand
D. Krofcheck

University of Canterbury, Christchurch, New Zealand
P. H. Butler

National Centre for Physics, Quaid-I-Azam University, Islamabad, Pakistan
A. Ahmad, M. Ahmad, Q. Hassan, H. R. Hoorani, W. A. Khan, A. Saddique, M. A. Shah, M. Shoaib, M. Waqas

National Centre for Nuclear Research, Swierk, Poland
H. Bialkowska, M. Bluj, B. Boimska, T. Frueboes, M. Górski, M. Kazana, K. Nawrocki, K. Romanowska-Rybinska, M. Szleper, P. Zalewski

Institute of Experimental Physics Faculty of Physics University of Warsaw, Warsaw, Poland
K. Bunkowski, A. Byszuk[36], K. Doroba, A. Kalinowski, M. Konecki, J. Krolikowski, M. Misiura, M. Olszewski, M. Walczak

Laboratório de Instrumentação e Física Experimental de Partículas, Lisbon, Portugal
P. Bargassa, C. Beirão Da Cruz E Silva, B. Calpas, A. Di Francesco, P. Faccioli, P. G. Ferreira Parracho, M. Gallinaro, J. Hollar, N. Leonardo, L. Lloret Iglesias, M. V. Nemallapudi, J. Rodrigues Antunes, J. Seixas, O. Toldaiev, D. Vadruccio, J. Varela

Joint Institute for Nuclear Research, Dubna, Russia
S. Afanasiev, P. Bunin, M. Gavrilenko, I. Golutvin, I. Gorbunov, A. Kamenev, V. Karjavin, A. Lanev, A. Malakhov, V. Matveev[37,38], V. Palichik, V. Perelygin, S. Shmatov, S. Shulha, N. Skatchkov, V. Smirnov, N. Voytishin, A. Zarubin

Petersburg Nuclear Physics Institute, Gatchina (St. Petersburg), Russia
L. Chtchipounov, V. Golovtsov, Y. Ivanov, V. Kim[39], E. Kuznetsova[40], V. Murzin, V. Oreshkin, V. Sulimov, A. Vorobyev

Institute for Nuclear Research, Moscow, Russia
Yu. Andreev, A. Dermenev, S. Gninenko, N. Golubev, A. Karneyeu, M. Kirsanov, N. Krasnikov, A. Pashenkov, D. Tlisov, A. Toropin

Institute for Theoretical and Experimental Physics, Moscow, Russia
V. Epshteyn, V. Gavrilov, N. Lychkovskaya, V. Popov, I. Pozdnyakov, G. Safronov, A. Spiridonov, M. Toms, E. Vlasov, A. Zhokin

Moscow Institute of Physics and Technology, Moscow, Russia
T. Aushev, A. Bylinkin[38]

National Research Nuclear University 'Moscow Engineering Physics Institute' (MEPhI), Moscow, Russia
R. Chistov[41], S. Polikarpov, E. Zhemchugov

P.N. Lebedev Physical Institute, Moscow, Russia
V. Andreev, M. Azarkin[38], I. Dremin[38], M. Kirakosyan, A. Leonidov[38], A. Terkulov

Skobeltsyn Institute of Nuclear Physics Lomonosov Moscow State University, Moscow, Russia
A. Baskakov, A. Belyaev, E. Boos, V. Bunichev, M. Dubinin[42], L. Dudko, A. Ershov, V. Klyukhin, N. Korneeva, I. Lokhtin, I. Miagkov, S. Obraztsov, M. Perfilov, V. Savrin, P. Volkov

Novosibirsk State University (NSU), Novosibirsk, Russia
V. Blinov[43], Y. Skovpen[43], D. Shtol[43]

State Research Center of Russian Federation Institute for High Energy Physics, Protvino, Russia
I. Azhgirey, I. Bayshev, S. Bitioukov, D. Elumakhov, V. Kachanov, A. Kalinin, D. Konstantinov, V. Krychkine, V. Petrov, R. Ryutin, A. Sobol, S. Troshin, N. Tyurin, A. Uzunian, A. Volkov

University of Belgrade Faculty of Physics and Vinca Institute of Nuclear Sciences, Belgrade, Serbia
P. Adzic[44], P. Cirkovic, D. Devetak, M. Dordevic, J. Milosevic, V. Rekovic

Centro de Investigaciones Energéticas Medioambientales y Tecnológicas (CIEMAT), Madrid, Spain
J. Alcaraz Maestre, M. Barrio Luna, E. Calvo, M. Cerrada, M. Chamizo Llatas, N. Colino, B. De La Cruz, A. Delgado Peris, A. Escalante Del Valle, C. Fernandez, J. P. Fernández Ramos, J. Flix, M. C. Fouz, P. Garcia-Abia, O. Gonzalez Lopez, S. Goy Lopez, J. M. Hernandez, M. I. Josa, E. Navarro De Martino, A. Pérez-Calero Yzquierdo, J. Puerta Pelayo, A. Quintario Olmeda, I. Redondo, L. Romero, M. S. Soares

Universidad Autónoma de Madrid, Madrid, Spain
J. F. de Trocóniz, M. Missiroli, D. Moran

Universidad de Oviedo, Oviedo, Spain
J. Cuevas, J. Fernandez Menendez, I. Gonzalez Caballero, J. R. González Fernández, E. Palencia Cortezon, S. Sanchez Cruz, I. Suárez Andrés, P. Vischia, J. M. Vizan Garcia

Instituto de Física de Cantabria (IFCA), CSIC-Universidad de Cantabria, Santander, Spain
I. J. Cabrillo, A. Calderon, E. Curras, M. Fernandez, J. Garcia-Ferrero, G. Gomez, A. Lopez Virto, J. Marco, C. Martinez Rivero, F. Matorras, J. Piedra Gomez, T. Rodrigo, A. Ruiz-Jimeno, L. Scodellaro, N. Trevisani, I. Vila, R. Vilar Cortabitarte

CERN, European Organization for Nuclear Research, Geneva, Switzerland
D. Abbaneo, E. Auffray, G. Auzinger, P. Baillon, A. H. Ball, D. Barney, P. Bloch, A. Bocci, C. Botta, T. Camporesi, R. Castello, M. Cepeda, G. Cerminara, Y. Chen, D. d'Enterria, A. Dabrowski, V. Daponte, A. David, M. De Gruttola, A. De Roeck, E. Di Marco[45], M. Dobson, B. Dorney, T. du Pree, D. Duggan, M. Dünser, N. Dupont, A. Elliott-Peisert, P. Everaerts, S. Fartoukh, G. Franzoni, J. Fulcher, W. Funk, D. Gigi, K. Gill, M. Girone, F. Glege, D. Gulhan, S. Gundacker, M. Guthoff, P. Harris, J. Hegeman, V. Innocente, P. Janot, J. Kieseler, H. Kirschenmann, V. Knünz, A. Kornmayer[16], M. J. Kortelainen, K. Kousouris, M. Krammer[1], C. Lange, P. Lecoq, C. Lourenço, M. T. Lucchini, L. Malgeri, M. Mannelli, A. Martelli, F. Meijers, J. A. Merlin, S. Mersi, E. Meschi, P. Milenovic[46], F. Moortgat, S. Morovic, M. Mulders, H. Neugebauer, S. Orfanelli, L. Orsini, L. Pape, E. Perez, M. Peruzzi, A. Petrilli, G. Petrucciani, A. Pfeiffer, M. Pierini, A. Racz, T. Reis, G. Rolandi[47], M. Rovere, H. Sakulin, J. B. Sauvan, C. Schäfer, C. Schwick, M. Seidel, A. Sharma, P. Silva, P. Sphicas[48], J. Steggemann, M. Stoye, Y. Takahashi, M. Tosi, D. Treille, A. Triossi, A. Tsirou, V. Veckalns[49], G. I. Veres[21], M. Verweij, N. Wardle, H. K. Wöhri, A. Zagozdzinska[36], W. D. Zeuner

Paul Scherrer Institut, Villigen, Switzerland
W. Bertl, K. Deiters, W. Erdmann, R. Horisberger, Q. Ingram, H. C. Kaestli, D. Kotlinski, U. Langenegger, T. Rohe, S. A. Wiederkehr

Institute for Particle Physics ETH Zurich, Zurich, Switzerland
F. Bachmair, L. Bäni, L. Bianchini, B. Casal, G. Dissertori, M. Dittmar, M. Donegà, C. Grab, C. Heidegger, D. Hits, J. Hoss, G. Kasieczka, W. Lustermann, B. Mangano, M. Marionneau, P. Martinez Ruiz del Arbol, M. Masciovecchio, M. T. Meinhard, D. Meister, F. Micheli, P. Musella, F. Nessi-Tedaldi, F. Pandolfi, J. Pata, F. Pauss, G. Perrin, L. Perrozzi, M. Quittnat, M. Rossini, M. Schönenberger, A. Starodumov[50], V. R. Tavolaro, K. Theofilatos, R. Wallny

Universität Zürich, Zurich, Switzerland
T. K. Aarrestad, C. Amsler[51], L. Caminada, M. F. Canelli, A. De Cosa, C. Galloni, A. Hinzmann, T. Hreus, B. Kilminster, J. Ngadiuba, D. Pinna, G. Rauco, P. Robmann, D. Salerno, C. Seitz, Y. Yang, A. Zucchetta

National Central University, Chung-Li, Taiwan
V. Candelise, T. H. Doan, Sh. Jain, R. Khurana, M. Konyushikhin, C. M. Kuo, W. Lin, A. Pozdnyakov, S. S. Yu

National Taiwan University (NTU), Taipei, Taiwan
Arun Kumar, P. Chang, Y. H. Chang, Y. Chao, K. F. Chen, P. H. Chen, F. Fiori, W. -S. Hou, Y. Hsiung, Y. F. Liu, R. -S. Lu, M. Miñano Moya, E. Paganis, A. Psallidas, J. f. Tsai

Chulalongkorn University Faculty of Science Department of Physics, Bangkok, Thailand
B. Asavapibhop, G. Singh, N. Sri manobhas, N. Suwonjandee

Physics Department Science and Art Faculty, Cukurova University, Adana, Turkey
A. Adiguzel, M. N. Bakirci[52], S. Damarseckin, Z. S. Demiroglu, C. Dozen, E. Eskut, S. Girgis, G. Gokbulut, Y. Guler, I. Hos[53], E. E. Kangal[54], O. Kara, U. Kiminsu, M. Oglakci, G. Onengut[55], K. Ozdemir[56], S. Ozturk[52], A. Polatoz, D. Sunar Cerci[57], S. Turkcapar, I. S. Zorbakir, C. Zorbilmez

Middle East Technical University Physics Department, Ankara, Turkey
B. Bilin, S. Bilmis, B. Isildak[58], G. Karapinar[59], M. Yalvac, M. Zeyrek

Bogazici University, Istanbul, Turkey
E. Gülmez, M. Kaya[60], O. Kaya[61], E. A. Yetkin[62], T. Yetkin[63]

Istanbul Technical University, Istanbul, Turkey
A. Cakir, K. Cankocak, S. Sen[64]

Institute for Scintillation Materials of National Academy of Science of Ukraine, Kharkov, Ukraine
B. Grynyov

National Scientific Center, Kharkov Institute of Physics and Technology, Kharkov, Ukraine
L. Levchuk, P. Sorokin

University of Bristol, Bristol, UK
R. Aggleton, F. Ball, L. Beck, J. J. Brooke, D. Burns, E. Clement, D. Cussans, H. Flacher, J. Goldstein, M. Grimes, G. P. Heath, H. F. Heath, J. Jacob, L. Kreczko, C. Lucas, D. M. Newbold[65], S. Paramesvaran, A. Poll, T. Sakuma, S. Seif El Nasr-storey, D. Smith, V. J. Smith

Rutherford Appleton Laboratory, Didcot, UK
K. W. Bell, A. Belyaev[66], C. Brew, R. M. Brown, L. Calligaris, D. Cieri, D. J. A. Cockerill, J. A. Coughlan, K. Harder, S. Harper, E. Olaiya, D. Petyt, C. H. Shepherd-Themistocleous, A. Thea, I. R. Tomalin, T. Williams

Imperial College, London, UK
M. Baber, R. Bainbridge, O. Buchmuller, A. Bundock, D. Burton, S. Casasso, M. Citron, D. Colling, L. Corpe, P. Dauncey, G. Davies, A. De Wit, M. Della Negra, R. Di Maria, P. Dunne, A. Elwood, D. Futyan, Y. Haddad, G. Hall, G. Iles, T. James, R. Lane, C. Laner, R. Lucas[65], L. Lyons, A.-M. Magnan, S. Malik, L. Mastrolorenzo, J. Nash, A. Nikitenko[50], J. Pela, B. Penning, M. Pesaresi, D. M. Raymond, A. Richards, A. Rose, E. Scott, C. Seez, S. Summers, A. Tapper, K. Uchida, M. Vazquez Acosta[67], T. Virdee[16], J. Wright, S. C. Zenz

Brunel University, Uxbridge, UK
J. E. Cole, P. R. Hobson, A. Khan, P. Kyberd, I. D. Reid, P. Symonds, L. Teodorescu, M. Turner

Baylor University, Waco, USA
A. Borzou, K. Call, J. Dittmann, K. Hatakeyama, H. Liu, N. Pastika

Catholic University of America, Washington, USA
R. Bartek, A. Dominguez

The University of Alabama, Tuscaloosa, USA
A. Buccilli, S. I. Cooper, C. Henderson, P. Rumerio, C. West

Boston University, Boston, USA
D. Arcaro, A. Avetisyan, T. Bose, D. Gastler, D. Rankin, C. Richardson, J. Rohlf, L. Sulak, D. Zou

Brown University, Providence, USA
G. Benelli, D. Cutts, A. Garabedian, J. Hakala, U. Heintz, J. M. Hogan, O. Jesus, K. H. M. Kwok, E. Laird, G. Landsberg, Z. Mao, M. Narain, S. Piperov, S. Sagir, E. Spencer, R. Syarif

University of California Davis, Davis, USA
R. Breedon, D. Burns, M. Calderon De La Barca Sanchez, S. Chauhan, M. Chertok, J. Conway, R. Conway, P. T. Cox, R. Erbacher, C. Flores, G. Funk, M. Gardner, W. Ko, R. Lander, C. Mclean, M. Mulhearn, D. Pellett, J. Pilot, S. Shalhout, M. Shi, J. Smith, M. Squires, D. Stolp, K. Tos, M. Tripathi

University of California, Los Angeles, USA
M. Bachtis, C. Bravo, R. Cousins, A. Dasgupta, A. Florent, J. Hauser, M. Ignatenko, N. Mccoll, D. Saltzberg, C. Schnaible, V. Valuev, M. Weber

University of California Riverside, Riverside, USA
E. Bouvier, K. Burt, R. Clare, J. Ellison, J. W. Gary, S. M. A. Ghiasi Shirazi, G. Hanson, J. Heilman, P. Jandir, E. Kennedy, F. Lacroix, O. R. Long, M. Olmedo Negrete, M. I. Paneva, A. Shrinivas, W. Si, H. Wei, S. Wimpenny, B. R. Yates

University of California San Diego, La Jolla, USA
J. G. Branson, G. B. Cerati, S. Cittolin, M. Derdzinski, R. Gerosa, A. Holzner, D. Klein, V. Krutelyov, J. Letts, I. Macneill, D. Olivito, S. Padhi, M. Pieri, M. Sani, V. Sharma, S. Simon, M. Tadel, A. Vartak, S. Wasserbaech[68], C. Welke, J. Wood, F. Würthwein, A. Yagil, G. Zevi Della Porta

University of California Santa Barbara - Department of Physics, Santa Barbara, USA
N. Amin, R. Bhandari, J. Bradmiller-Feld, C. Campagnari, A. Dishaw, V. Dutta, M. Franco Sevilla, C. George, F. Golf, L. Gouskos, J. Gran, R. Heller, J. Incandela, S. D. Mullin, A. Ovcharova, H. Qu, J. Richman, D. Stuart, I. Suarez, J. Yoo

California Institute of Technology, Pasadena, USA
D. Anderson, J. Bendavid, A. Bornheim, J. Bunn, J. Duarte, J. M. Lawhorn, A. Mott, H. B. Newman, C. Pena, M. Spiropulu, J. R. Vlimant, S. Xie, R. Y. Zhu

Carnegie Mellon University, Pittsburgh, USA
M. B. Andrews, T. Ferguson, M. Paulini, J. Russ, M. Sun, H. Vogel, I. Vorobiev, M. Weinberg

University of Colorado Boulder, Boulder, USA
J. P. Cumalat, W. T. Ford, F. Jensen, A. Johnson, M. Krohn, S. Leontsinis, T. Mulholland, K. Stenson, S. R. Wagner

Cornell University, Ithaca, USA
J. Alexander, J. Chaves, J. Chu, S. Dittmer, K. Mcdermott, N. Mirman, G. Nicolas Kaufman, J. R. Patterson, A. Rinkevicius, A. Ryd, L. Skinnari, L. Soffi, S. M. Tan, Z. Tao, J. Thom, J. Tucker, P. Wittich, M. Zientek

Fairfield University, Fairfield, USA
D. Winn

Fermi National Accelerator Laboratory, Batavia, USA
S. Abdullin, M. Albrow, G. Apollinari, A. Apresyan, S. Banerjee, L. A. T. Bauerdick, A. Beretvas, J. Berryhill, P. C. Bhat, G. Bolla, K. Burkett, J. N. Butler, H. W. K. Cheung, F. Chlebana, S. Cihangir†, M. Cremonesi, V. D. Elvira, I. Fisk, J. Freeman, E. Gottschalk, L. Gray, D. Green, S. Grünendahl, O. Gutsche, D. Hare, R. M. Harris, S. Hasegawa, J. Hirschauer, Z. Hu, B. Jayatilaka, S. Jindariani, M. Johnson, U. Joshi, B. Klima, B. Kreis, S. Lammel, J. Linacre,

D. Lincoln, R. Lipton, M. Liu, T. Liu, R. Lopes De Sá, J. Lykken, K. Maeshima, N. Magini, J. M. Marraffino, S. Maruyama, D. Mason, P. McBride, P. Merkel, S. Mrenna, S. Nahn, V. O'Dell, K. Pedro, O. Prokofyev, G. Rakness, L. Ristori, E. Sexton-Kennedy, A. Soha, W. J. Spalding, L. Spiegel, S. Stoynev, J. Strait, N. Strobbe, L. Taylor, S. Tkaczyk, N. V. Tran, L. Uplegger, E. W. Vaandering, C. Vernieri, M. Verzocchi, R. Vidal, M. Wang, H. A. Weber, A. Whitbeck, Y. Wu

University of Florida, Gainesville, USA
D. Acosta, P. Avery, P. Bortignon, D. Bourilkov, A. Brinkerhoff, A. Carnes, M. Carver, D. Curry, S. Das, R. D. Field, I. K. Furic, J. Konigsberg, A. Korytov, J. F. Low, P. Ma, K. Matchev, H. Mei, G. Mitselmakher, D. Rank, L. Shchutska, D. Sperka, L. Thomas, J. Wang, S. Wang, J. Yelton

Florida International University, Miami, USA
S. Linn, P. Markowitz, G. Martinez, J. L. Rodriguez

Florida State University, Tallahassee, USA
A. Ackert, T. Adams, A. Askew, S. Bein, S. Hagopian, V. Hagopian, K. F. Johnson, T. Kolberg, H. Prosper, A. Santra, R. Yohay

Florida Institute of Technology, Melbourne, USA
M. M. Baarmand, V. Bhopatkar, S. Colafranceschi, M. Hohlmann, D. Noonan, T. Roy, F. Yumiceva

University of Illinois at Chicago (UIC), Chicago, USA
M. R. Adams, L. Apanasevich, D. Berry, R. R. Betts, I. Bucinskaite, R. Cavanaugh, O. Evdokimov, L. Gauthier, C. E. Gerber, D. J. Hofman, K. Jung, I. D. Sandoval Gonzalez, N. Varelas, H. Wang, Z. Wu, M. Zakaria, J. Zhang

The University of Iowa, Iowa City, USA
B. Bilki[69], W. Clarida, K. Dilsiz, S. Durgut, R. P. Gandrajula, M. Haytmyradov, V. Khristenko, J.-P. Merlo, H. Mermerkaya[70], A. Mestvirishvili, A. Moeller, J. Nachtman, H. Ogul, Y. Onel, F. Ozok[71], A. Penzo, C. Snyder, E. Tiras, J. Wetzel, K. Yi

Johns Hopkins University, Baltimore, USA
B. Blumenfeld, A. Cocoros, N. Eminizer, D. Fehling, L. Feng, A. V. Gritsan, P. Maksimovic, J. Roskes, U. Sarica, M. Swartz, M. Xiao, C. You

The University of Kansas, Lawrence, USA
A. Al-bataineh, P. Baringer, A. Bean, S. Boren, J. Bowen, J. Castle, L. Forthomme, R. P. Kenny III, S. Khalil, A. Kropivnitskaya, D. Majumder, W. Mcbrayer, M. Murray, S. Sanders, R. Stringer, J. D. Tapia Takaki, Q. Wang

Kansas State University, Manhattan, USA
A. Ivanov, K. Kaadze, Y. Maravin, A. Mohammadi, L. K. Saini, N. Skhirtladze, S. Toda

Lawrence Livermore National Laboratory, Livermore, USA
F. Rebassoo, D. Wright

University of Maryland, College Park, USA
C. Anelli, A. Baden, O. Baron, A. Belloni, B. Calvert, S. C. Eno, C. Ferraioli, J. A. Gomez, N. J. Hadley, S. Jabeen, G. Y. Jeng, R. G. Kellogg, J. Kunkle, A. C. Mignerey, F. Ricci-Tam, Y. H. Shin, A. Skuja, M. B. Tonjes, S. C. Tonwar

Massachusetts Institute of Technology, Cambridge, USA
D. Abercrombie, B. Allen, A. Apyan, V. Azzolini, R. Barbieri, A. Baty, R. Bi, K. Bierwagen, S. Brandt, W. Busza, I. A. Cali, M. D'Alfonso, Z. Demiragli, G. Gomez Ceballos, M. Goncharov, D. Hsu, Y. Iiyama, G. M. Innocenti, M. Klute, D. Kovalskyi, K. Krajczar, Y. S. Lai, Y.-J. Lee, A. Levin, P. D. Luckey, B. Maier, A. C. Marini, C. Mcginn, C. Mironov, S. Narayanan, X. Niu, C. Paus, C. Roland, G. Roland, J. Salfeld-Nebgen, G. S. F. Stephans, K. Tatar, D. Velicanu, J. Wang, T. W. Wang, B. Wyslouch

University of Minnesota, Minneapolis, USA
A. C. Benvenuti, R. M. Chatterjee, A. Evans, P. Hansen, S. Kalafut, S. C. Kao, Y. Kubota, Z. Lesko, J. Mans, S. Nourbakhsh, N. Ruckstuhl, R. Rusack, N. Tambe, J. Turkewitz

University of Mississippi, Oxford, USA
J. G. Acosta, S. Oliveros

University of Nebraska-Lincoln, Lincoln, USA
E. Avdeeva, K. Bloom, D. R. Claes, C. Fangmeier, R. Gonzalez Suarez, R. Kamalieddin, I. Kravchenko, A. Malta Rodrigues, J. Monroy, J. E. Siado, G. R. Snow, B. Stieger

State University of New York at Buffalo, Buffalo, USA
M. Alyari, J. Dolen, A. Godshalk, C. Harrington, I. Iashvili, J. Kaisen, D. Nguyen, A. Parker, S. Rappoccio, B. Roozbahani

Northeastern University, Boston, USA
G. Alverson, E. Barberis, A. Hortiangtham, A. Massironi, D. M. Morse, D. Nash, T. Orimoto, R. Teixeira De Lima, D. Trocino, R.-J. Wang, D. Wood

Northwestern University, Evanston, USA
S. Bhattacharya, O. Charaf, K. A. Hahn, A. Kumar, N. Mucia, N. Odell, B. Pollack, M. H. Schmitt, K. Sung, M. Trovato, M. Velasco

University of Notre Dame, Notre Dame, USA
N. Dev, M. Hildreth, K. Hurtado Anampa, C. Jessop, D. J. Karmgard, N. Kellams, K. Lannon, N. Marinelli, F. Meng, C. Mueller, Y. Musienko[37], M. Planer, A. Reinsvold, R. Ruchti, N. Rupprecht, G. Smith, S. Taroni, M. Wayne, M. Wolf, A. Woodard

The Ohio State University, Columbus, USA
J. Alimena, L. Antonelli, B. Bylsma, L. S. Durkin, S. Flowers, B. Francis, A. Hart, C. Hill, R. Hughes, W. Ji, B. Liu, W. Luo, D. Puigh, B. L. Winer, H. W. Wulsin

Princeton University, Princeton, USA
S. Cooperstein, O. Driga, P. Elmer, J. Hardenbrook, P. Hebda, D. Lange, J. Luo, D. Marlow, T. Medvedeva, K. Mei, I. Ojalvo, J. Olsen, C. Palmer, P. Piroué, D. Stickland, A. Svyatkovskiy, C. Tully

University of Puerto Rico, Mayaguez, USA
S. Malik

Purdue University, West Lafayette, USA
A. Barker, V. E. Barnes, S. Folgueras, L. Gutay, M. K. Jha, M. Jones, A. W. Jung, A. Khatiwada, D. H. Miller, N. Neumeister, J. F. Schulte, X. Shi, J. Sun, F. Wang, W. Xie

Purdue University Northwest, Hammond, USA
N. Parashar, J. Stupak

Rice University, Houston, USA
A. Adair, B. Akgun, Z. Chen, K. M. Ecklund, F. J. M. Geurts, M. Guilbaud, W. Li, B. Michlin, M. Northup, B. P. Padley, J. Roberts, J. Rorie, Z. Tu, J. Zabel

University of Rochester, Rochester, USA
B. Betchart, A. Bodek, P. de Barbaro, R. Demina, Y.t. Duh, T. Ferbel, M. Galanti, A. Garcia-Bellido, J. Han, O. Hindrichs, A. Khukhunaishvili, K. H. Lo, P. Tan, M. Verzetti

Rutgers, The State University of New Jersey, Piscataway, USA
A. Agapitos, J. P. Chou, Y. Gershtein, T. A. Gómez Espinosa, E. Halkiadakis, M. Heindl, E. Hughes, S. Kaplan, R. Kunnawalkam Elayavalli, S. Kyriacou, A. Lath, K. Nash, M. Osherson, H. Saka, S. Salur, S. Schnetzer, D. Sheffield, S. Somalwar, R. Stone, S. Thomas, P. Thomassen, M. Walker

University of Tennessee, Knoxville, USA
A. G. Delannoy, M. Foerster, J. Heideman, G. Riley, K. Rose, S. Spanier, K. Thapa

Texas A&M University, College Station, USA
O. Bouhali[72], A. Celik, M. Dalchenko, M. De Mattia, A. Delgado, S. Dildick, R. Eusebi, J. Gilmore, T. Huang, E. Juska, T. Kamon[73], R. Mueller, Y. Pakhotin, R. Patel, A. Perloff, L. Perniè, D. Rathjens, A. Safonov, A. Tatarinov, K. A. Ulmer

Texas Tech University, Lubbock, USA
N. Akchurin, C. Cowden, J. Damgov, F. De Guio, C. Dragoiu, P. R. Dudero, J. Faulkner, E. Gurpinar, S. Kunori, K. Lamichhane, S. W. Lee, T. Libeiro, T. Peltola, S. Undleeb, I. Volobouev, Z. Wang

Vanderbilt University, Nashville, USA
S. Greene, A. Gurrola, R. Janjam, W. Johns, C. Maguire, A. Melo, H. Ni, P. Sheldon, S. Tuo, J. Velkovska, Q. Xu

University of Virginia, Charlottesville, USA
M. W. Arenton, P. Barria, B. Cox, J. Goodell, R. Hirosky, A. Ledovskoy, H. Li, C. Neu, T. Sinthuprasith, X. Sun, Y. Wang, E. Wolfe, F. Xia

Wayne State University, Detroit, USA
C. Clarke, R. Harr, P. E. Karchin, J. Sturdy

University of Wisconsin-Madison, Madison, WI, USA
D. A. Belknap, J. Buchanan, C. Caillol, S. Dasu, L. Dodd, S. Duric, B. Gomber, M. Grothe, M. Herndon, A. Hervé, P. Klabbers, A. Lanaro, A. Levine, K. Long, R. Loveless, T. Perry, G. A. Pierro, G. Polese, T. Ruggles, A. Savin, N. Smith, W. H. Smith, D. Taylor, N. Woods

† **Deceased**

1: Also at Vienna University of Technology, Vienna, Austria
2: Also at State Key Laboratory of Nuclear Physics and Technology, Peking University, Beijing, China
3: Also at Institut Pluridisciplinaire Hubert Curien (IPHC), Université de Strasbourg, CNRS/IN2P3, Strasbourg, France
4: Also at Universidade Estadual de Campinas, Campinas, Brazil
5: Also at Universidade Federal de Pelotas, Pelotas, Brazil
6: Also at Université Libre de Bruxelles, Bruxelles, Belgium
7: Also at Deutsches Elektronen-Synchrotron, Hamburg, Germany
8: Also at Joint Institute for Nuclear Research, Dubna, Russia
9: Also at Helwan University, Cairo, Egypt
10: Now at Zewail City of Science and Technology, Zewail, Egypt
11: Now at Fayoum University, El-Fayoum, Egypt
12: Also at British University in Egypt, Cairo, Egypt
13: Now at Ain Shams University, Cairo, Egypt
14: Also at Université de Haute Alsace, Mulhouse, France
15: Also at Skobeltsyn Institute of Nuclear Physics, Lomonosov Moscow State University, Moscow, Russia
16: Also at CERN, European Organization for Nuclear Research, Geneva, Switzerland
17: Also at RWTH Aachen University, III. Physikalisches Institut A, Aachen, Germany
18: Also at University of Hamburg, Hamburg, Germany
19: Also at Brandenburg University of Technology, Cottbus, Germany
20: Also at Institute of Nuclear Research ATOMKI, Debrecen, Hungary
21: Also at MTA-ELTE Lendület CMS Particle and Nuclear Physics Group, Eötvös Loránd University, Budapest, Hungary
22: Also at Institute of Physics, University of Debrecen, Debrecen, Hungary
23: Also at Indian Institute of Technology Bhubaneswar, Bhubaneswar, India
24: Also at University of Visva-Bharati, Santiniketan, India
25: Also at Indian Institute of Science Education and Research, Bhopal, India
26: Also at Institute of Physics, Bhubaneswar, India
27: Also at University of Ruhuna, Matara, Sri Lanka
28: Also at Isfahan University of Technology, Isfahan, Iran
29: Also at Yazd University, Yazd, Iran
30: Also at Plasma Physics Research Center, Science and Research Branch, Islamic Azad University, Tehran, Iran
31: Also at Università degli Studi di Siena, Siena, Italy
32: Also at Purdue University, West Lafayette, USA
33: Also at International Islamic University of Malaysia, Kuala Lumpur, Malaysia
34: Also at Malaysian Nuclear Agency, MOSTI, Kajang, Malaysia
35: Also at Consejo Nacional de Ciencia y Tecnología, Mexico city, Mexico

36: Also at Warsaw University of Technology, Institute of Electronic Systems, Warsaw, Poland
37: Also at Institute for Nuclear Research, Moscow, Russia
38: Now at National Research Nuclear University 'Moscow Engineering Physics Institute' (MEPhI), Moscow, Russia
39: Also at St. Petersburg State Polytechnical University, St. Petersburg, Russia
40: Also at University of Florida, Gainesville, USA
41: Also at P.N. Lebedev Physical Institute, Moscow, Russia
42: Also at California Institute of Technology, Pasadena, USA
43: Also at Budker Institute of Nuclear Physics, Novosibirsk, Russia
44: Also at Faculty of Physics, University of Belgrade, Belgrade, Serbia
45: Also at INFN Sezione di Roma; Università di Roma, Rome, Italy
46: Also at University of Belgrade, Faculty of Physics and Vinca Institute of Nuclear Sciences, Belgrade, Serbia
47: Also at Scuola Normale e Sezione dell'INFN, Pisa, Italy
48: Also at National and Kapodistrian University of Athens, Athens, Greece
49: Also at Riga Technical University, Riga, Latvia
50: Also at Institute for Theoretical and Experimental Physics, Moscow, Russia
51: Also at Albert Einstein Center for Fundamental Physics, Bern, Switzerland
52: Also at Gaziosmanpasa University, Tokat, Turkey
53: Also at Istanbul Aydin University, Istanbul, Turkey
54: Also at Mersin University, Mersin, Turkey
55: Also at Cag University, Mersin, Turkey
56: Also at Piri Reis University, Istanbul, Turkey
57: Also at Adiyaman University, Adiyaman, Turkey
58: Also at Ozyegin University, Istanbul, Turkey
59: Also at Izmir Institute of Technology, Izmir, Turkey
60: Also at Marmara University, Istanbul, Turkey
61: Also at Kafkas University, Kars, Turkey
62: Also at Istanbul Bilgi University, Istanbul, Turkey
63: Also at Yildiz Technical University, Istanbul, Turkey
64: Also at Hacettepe University, Ankara, Turkey
65: Also at Rutherford Appleton Laboratory, Didcot, UK
66: Also at School of Physics and Astronomy, University of Southampton, Southampton, UK
67: Also at Instituto de Astrofísica de Canarias, La Laguna, Spain
68: Also at Utah Valley University, Orem, USA
69: Also at Argonne National Laboratory, Argonne, USA
70: Also at Erzincan University, Erzincan, Turkey
71: Also at Mimar Sinan University, Istanbul, Istanbul, Turkey
72: Also at Texas A&M University at Qatar, Doha, Qatar
73: Also at Kyungpook National University, Taegu, Korea